Introduction to nanofabrication

Enzo Di Fabrizio

L.I.LIT

Laboratory
for
Interdisciplanry
LIThography

LILIT beamline INFM (National Institute for Matter Physics)
@ Elettra Synchrotron Light Source
-S.S 14 Km 163.5, Area Science Park, 34012 Basovizza- Trieste (Italy)

Lesson plan

- Lesson 1: introduction to nanofabrication
- Lesson 2: diffractive optics and X-ray microscopy
- Lesson 3: 3D fabrication and optical manipulation and spectrosopy

ELETTRA

TASC National Laboratory of INFM

Why reduce the sizes?

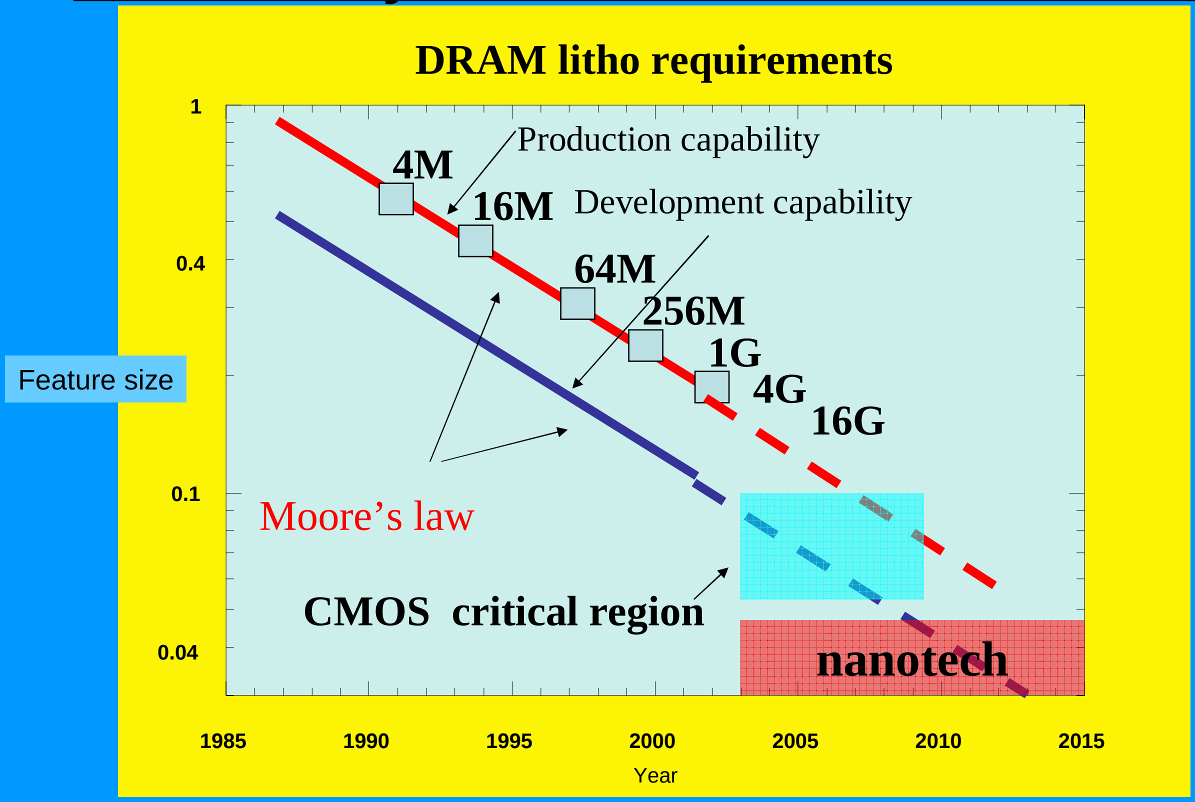

Lithographic techniques

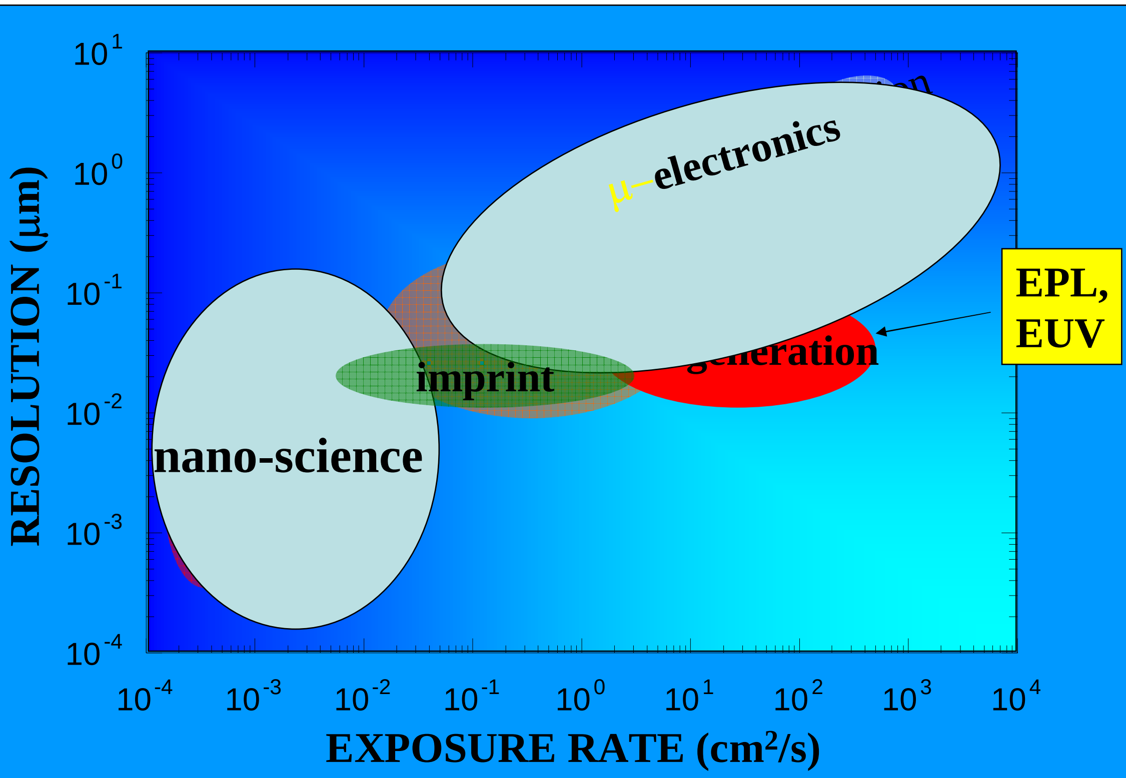

The scale length of things

“Objects” from nature

Arificial objects

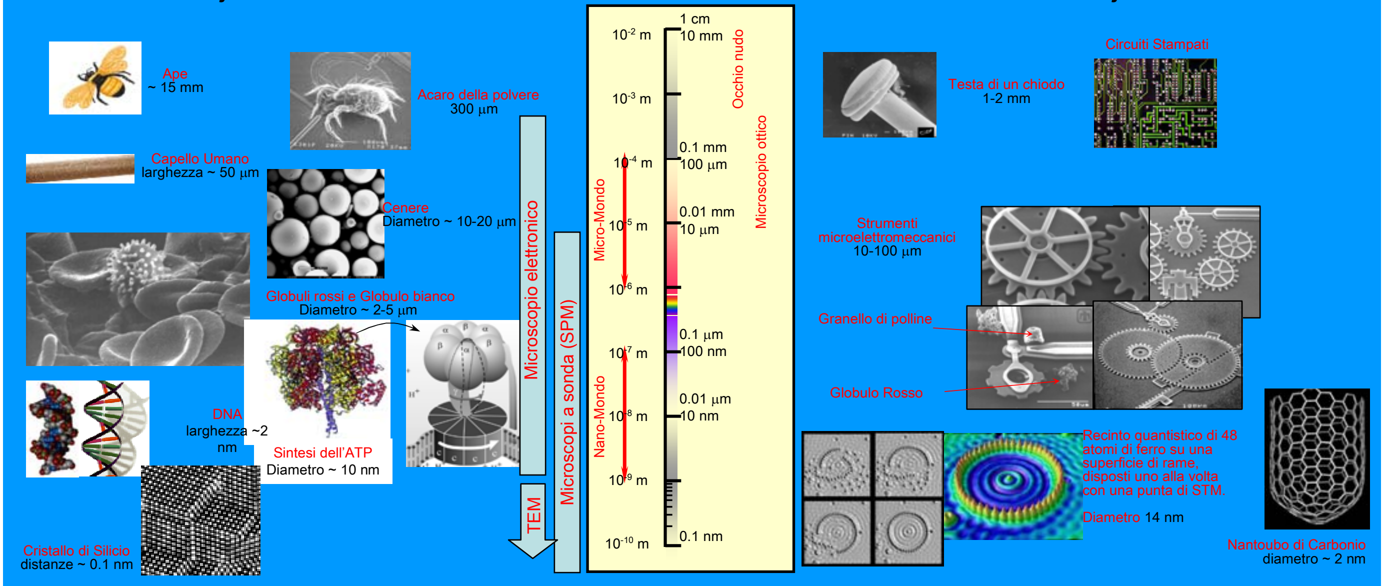

Ape
~ 15 mm

Acaro della polvere
300 µm

Capello Umano
larghezza ~ 50 µm

Cenere
Diametro ~ 10-20 µm

Globuli rossi e Globulo bianco
Diametro ~ 2-5 µm

DNA
larghezza ~2 nm

Sintesi dell'ATP
Diametro ~ 10 nm

Cristallo di Silicio
distanze ~ 0.1 nm

Microscopio elettronico

Microscopi a sonda (SPM)

TEM

10^{-2} m — 1 cm, 10 mm
10^{-3} m
10^{-4} m — 0.1 mm, 100 µm
10^{-5} m — 0.01 mm, 10 µm
10^{-6} m
10^{-7} m — 0.1 µm, 100 nm
10^{-8} m — 0.01 µm, 10 nm
10^{-9} m
10^{-10} m — 0.1 nm

Micro-Mondo

Nano-Mondo

Occhio nudo

Microscopio ottico

Testa di un chiodo
1-2 mm

Circuiti Stampati

Strumenti microelettromeccanici
10-100 µm

Granello di polline

Globulo Rosso

Recinto quantistico di 48 atomi di ferro su una superficie di rame, disposti uno alla volta con una punta di STM.

Diametro 14 nm

Nantoubo di Carbonio
diametro ~ 2 nm

Tools to observe the nano world

- (SPM, scanning probe microscope):

  STM (scanning tunneling microscope) Resolution ~0.1 nm

  AFM (atomic force microscope) Resolution ~1 0nm

- SEM (scanning electron microscope) Resolution ~1 nm

- TEM (transmission electron microscope) Resolution ~0.1 nm

STM microscope

Muovendo la punta sopra la superficie, si misura la corrente di elettroni che che passano dallla superficie alla punta (o viceversa) per effetto tunnel. Spostando la punta con dei piezoelettrici (precisione 0.01 nm) si ottiene una mappa della densita' elettronica.

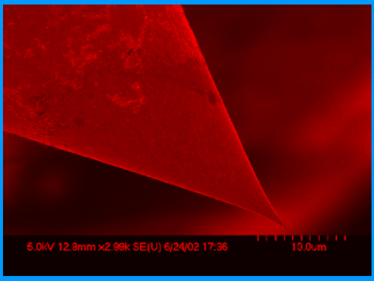

Immagine di una punta
per STM

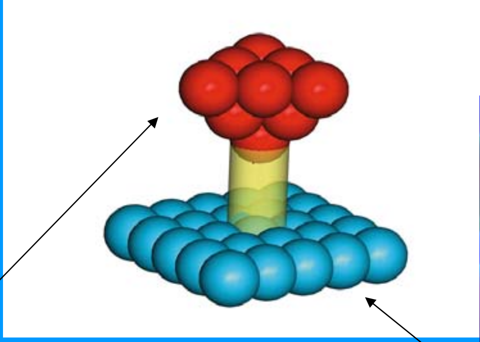

Densita' elettronica di una superficie di Nickel (110).
Realizzazione ed elaborazione IBM

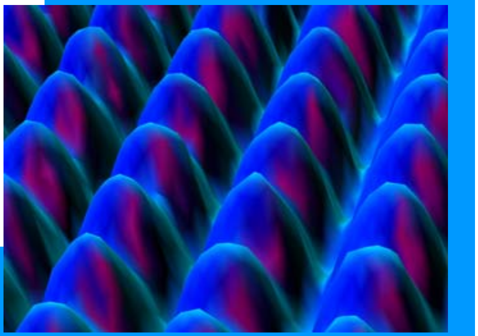

AFM microscope

Muovendo la punta sopra il campione, si misura il piegamento della piccola leva (canti-lever) dovuto alle forze di interazione atomiche e molecolari.

Si ottiene una immagine topografica della superficie che consente di misurare anche materiali isolanti (organici, biologici)

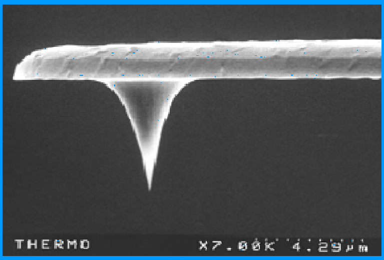

Immagine di una punta
montata su una piccola leva
per AFM

Topografia della superficie di globuli rossi.

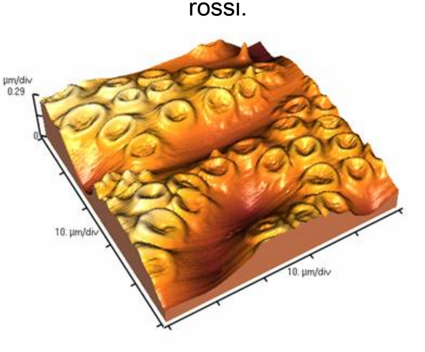

ZnSe/GaAs heterostructure

TEM at the Centre for Electron Microscopy

Elvio Carlino
Centro di Microscopia Elettronica - INFM - TASC

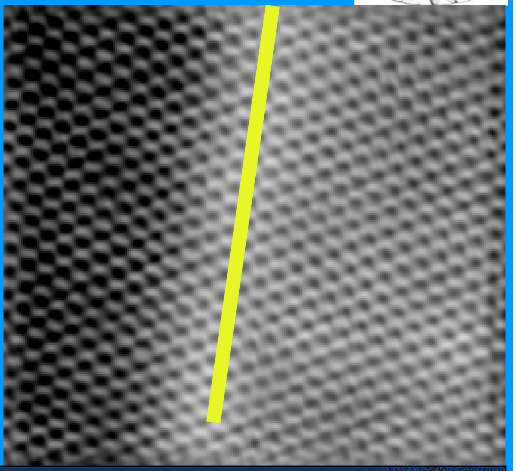

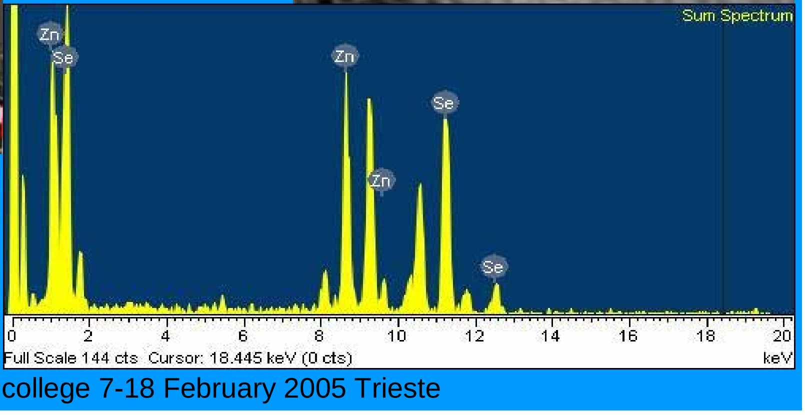

Lithography Techniques for Nanofabrication

- Fundamentals of Lithography
- Beam Lithography
- Alternate Nanolithography Techniques

Fundamentals of Lithography

The Si revolution…

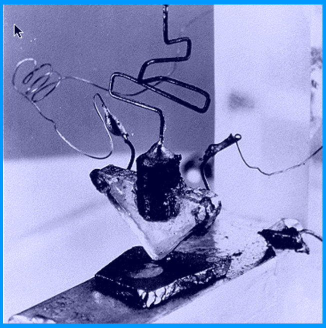

First Transistor
Bell Labs (1947)

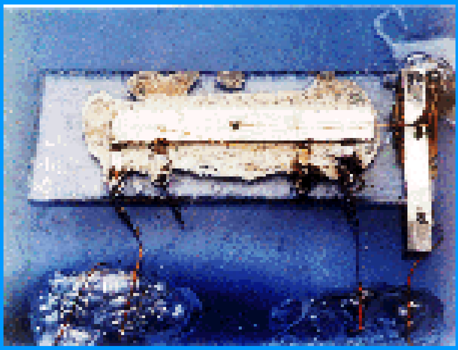

Si integrated circuits
Texas Instruments (~1960)

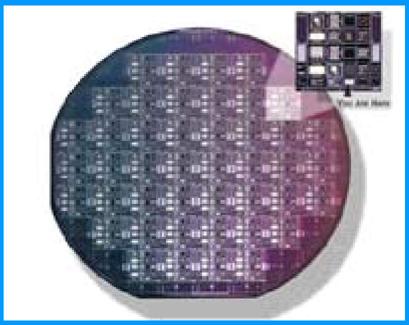

Modern ICs

More ? Check out:
http://www.pbs.org/transistor/background1/events/miraclemo.html
http://www.ti.com/corp/docs/company/history/firstic.shtml

The need of micropatterning

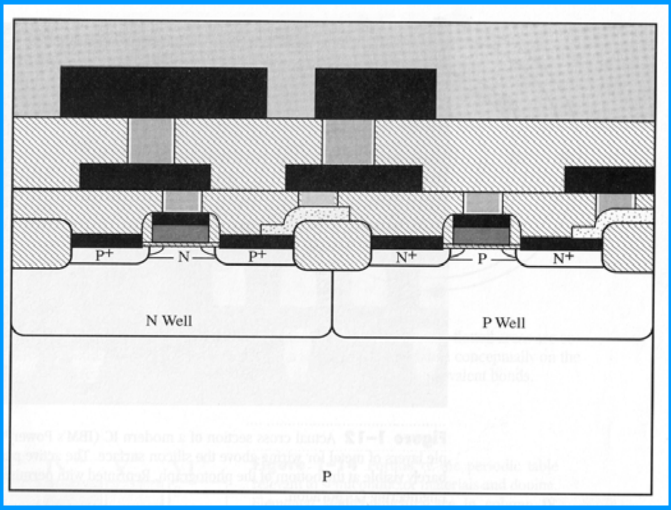

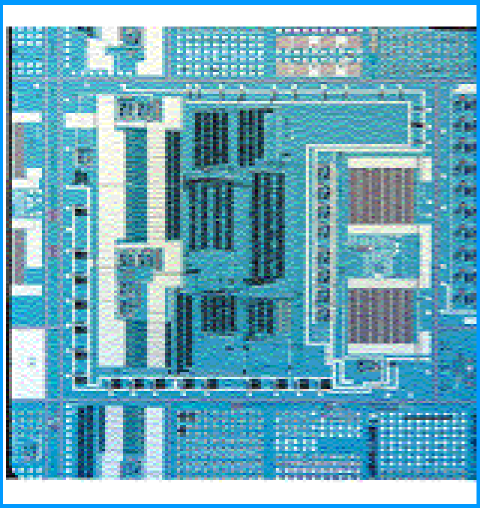

The batch fabrication of microstructures requires a low-cost, high throughput surface patterning technology

---

Elements of photolithography

- ***Lithography*** **consists of patterning a substrate by employing the interaction of beams of photons or particles with materials.**
- ***Photolithography*** **is widely used in the integrated circuits (ICs) manufacturing.**
- **The process of IC manufacturing consists of a series of 10-30 steps or more, called *mask layers* where layers of materials coated with resists are patterned then transferred onto the material layer.**

Elements of photolithography (ctnd.)

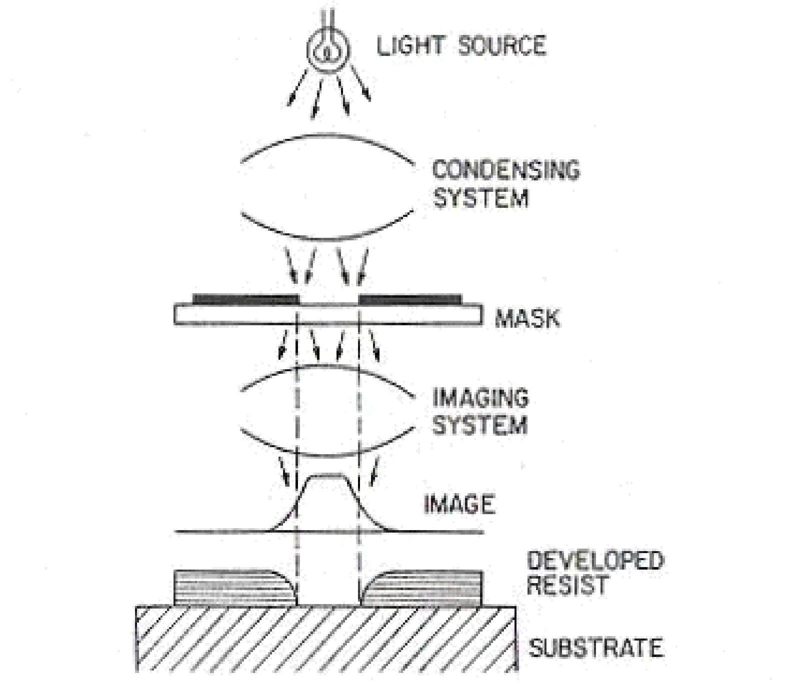

Output Spectrum of Hg Arc Lamp

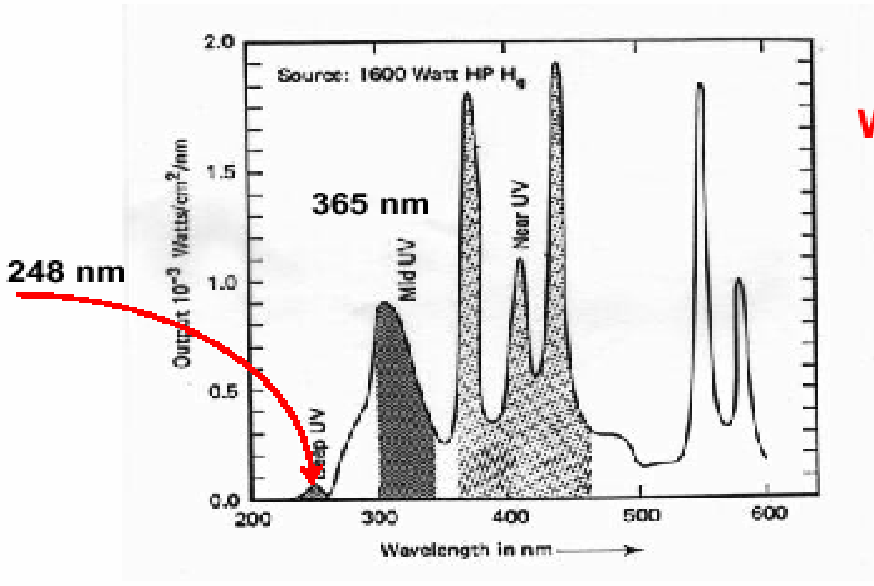

$R = k_1\lambda/NA$

Changing Wavelengths

248 nm
193 nm
157 nm
EUV (13 nm)
X-ray

Size Scales Accessible to Nanofabrication Approach

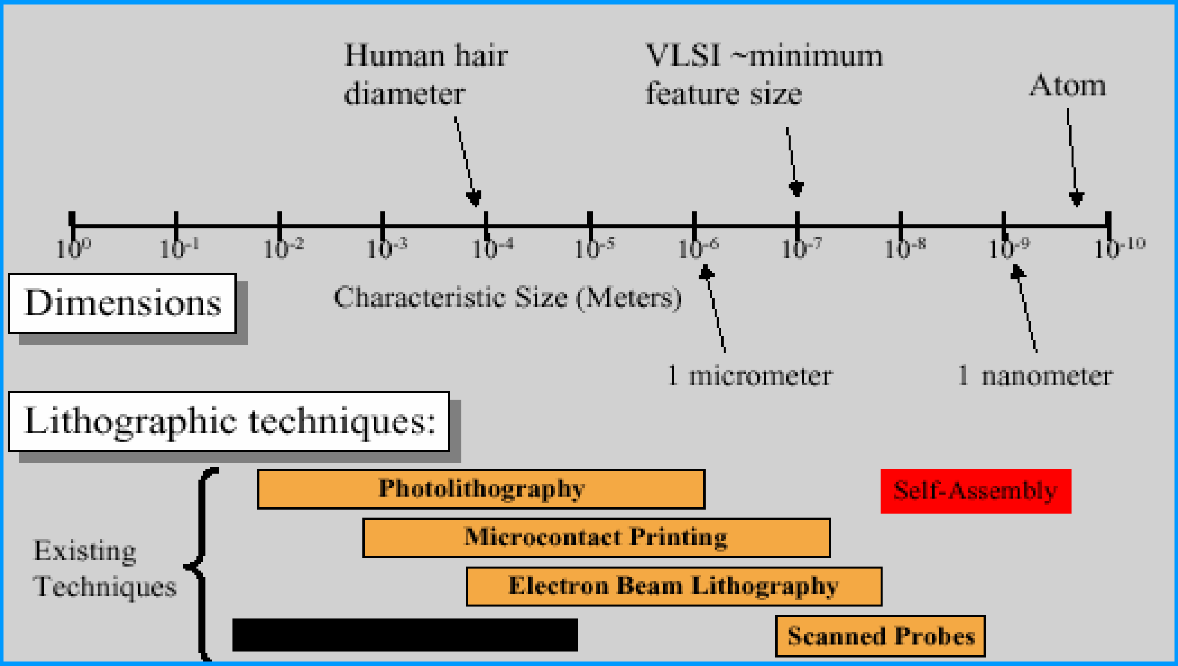

Human hair diameter

VLSI ~minimum feature size

Atom

10^{0} 10^{-1} 10^{-2} 10^{-3} 10^{-4} 10^{-5} 10^{-6} 10^{-7} 10^{-8} 10^{-9} 10^{-10}

Dimensions

Characteristic Size (Meters)

1 micrometer

1 nanometer

Lithographic techniques:

Existing Techniques

- **Photolithography**
- **Self-Assembly**
- **Microcontact Printing**
- **Electron Beam Lithography**
- [redacted]
- **Scanned Probes**

Elements of photolithography (ctnd.)

- **A photolithography system consists of a light source, a mask, and a optical projection system.**
- ***Photoresists*** **are radiation sensitive materials that usually consist of a photo-sensitive compound, a polymeric backbone, and a solvent.**
- **Resists can be classified upon their solubility after exposure into:** ***positive resists*** **(solubility of exposed area increases) and** ***negative resists*** **(solubility of exposed area decreases).**

Types of photolithography

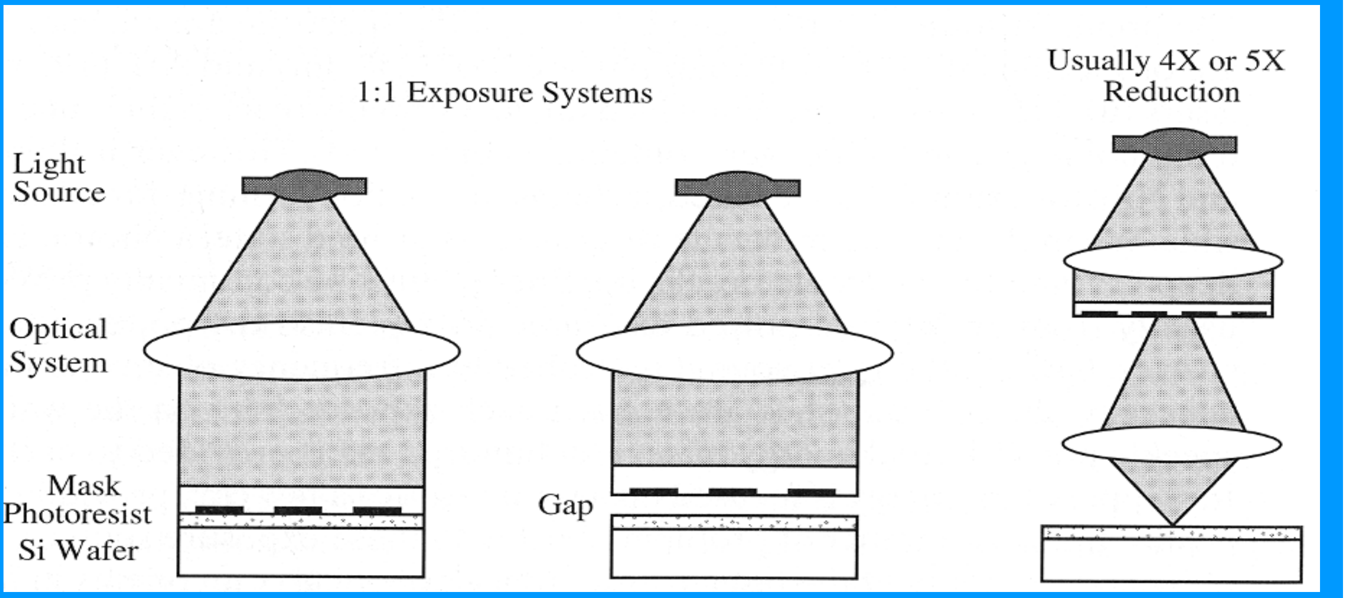

Contact Printing **Proximity Printing** **Projection Printing**

Micro- and nanolithography

- Present techniques in IC manufacturing involve dimensions in order of 100-150 nm.
- Diffraction and other optical effects limit the resolution of “standard” UV photolithography to the ~100 nm range.
- Photolithography continues to support IC manufacturing in the sub-100 nm region through continuous advances in optics (UV to DUV to EUV) and resist engineering.
- Exploratory research in the sub-100 nm region may also be accomplished through alternate patterning techniques such as *x-ray-*, *ion-* and *electron beam-* lithography.

BEAM ASSISTED LITHOGRAPHY

- X-ray
- Electron Beam
- Ion Beam

X-Ray lithography

- Diffraction limits lithography resolution to $\lambda/2$
- Obvious solution: use lower wavelengths sources
- DUV and EUV approaching standardization
- X-Ray lithography still posing no threat to optical

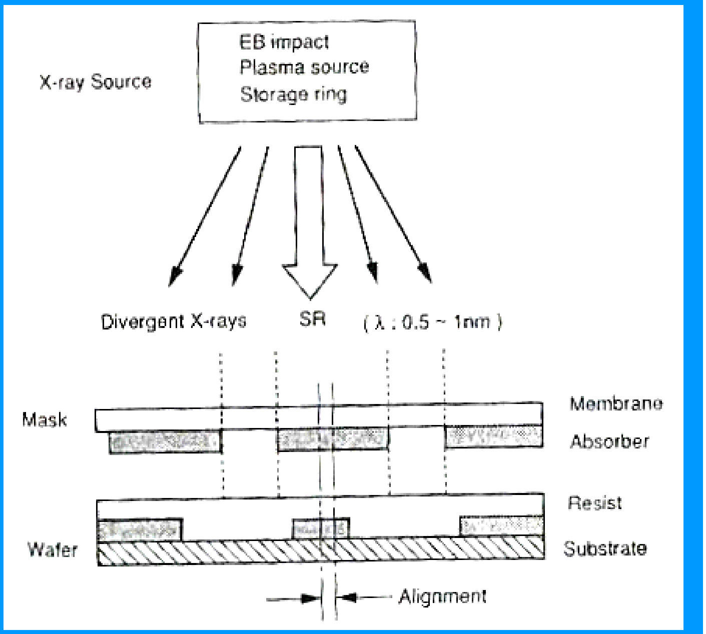

X Rays

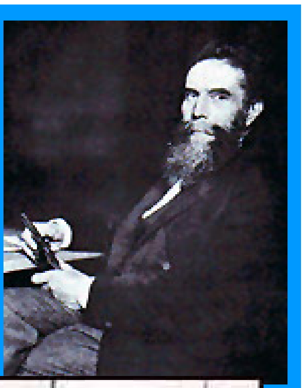

Features:

- **Discovered by Wilhelm Conrad Röntgen in 1895**
- **Experiments in a vacuum tube made a nearby fluorescent screen glow.**

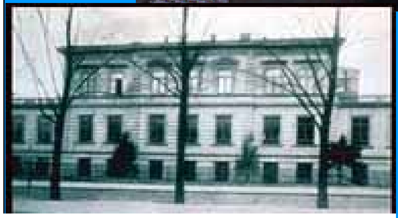

1901 **W. C. Roentgen** in Physics for the discovery of x-rays.
1914 **M. von Laue** in Physics for x-ray diffraction from crystals.
1915 **W. H. Bragg and W. L. Bragg** in Physics for crystal structure derived from x-ray diffraction.
1917 **C. G. Barkla** in Physics for characteristic radiation of elements.
1924 **K. M. G. Siegbahn** in Physics for x-ray spectroscopy.
1927 **A. H. Compton** in Physics for scattering of x-rays by electrons.
1936 **P. Debye** in Chemistry for diffraction of x-rays and electrons in gases.
1962 **M. Perutz and J. Kendrew** in Chemistry for the structure of hemoglobin.
1962 **J. Watson, M. Wilkins, and F. Crick** in Medicine for the structure of DNA.
1979 **A. McLeod Cormack and G. Newbold Hounsfield** in Medicine for computed axial tomography.
1981 **K. M. Siegbahn** in Physics for high resolution electron spectroscopy.
1985 **H. Hauptman and J. Karle** in Chemistry for direct methods to determine x-ray structures.
1988 **J. Deisenhofer, R. Huber, and H. Michel** in Chemistry for the structures of proteins that are crucial to photosynthesis.

X Rays

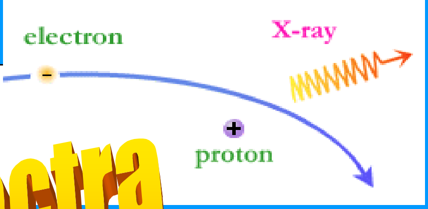

Methods of production:

- **acceleration of free electrons**
  - X ray tubes
  - accelerators

Continuous spectra

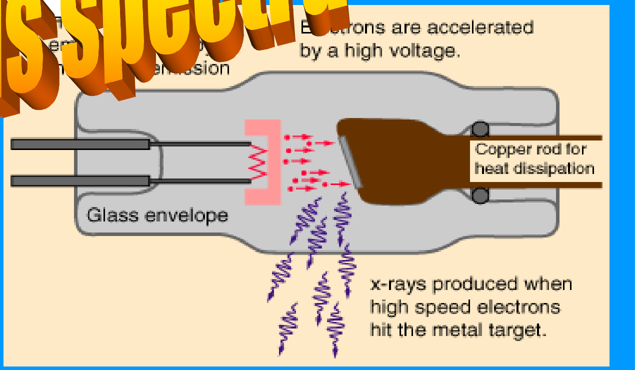

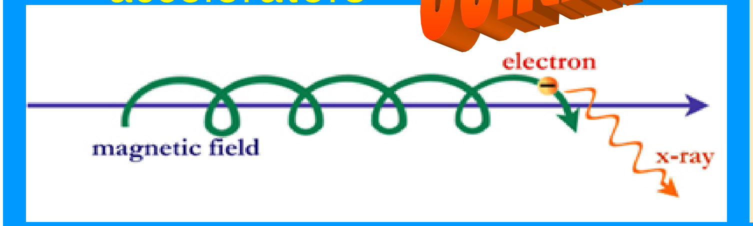

- Excitation of atomic electrons

Discrete spectra

THEORETICAL UNDERSTANDING →

1873 **Maxwell's equations**

→ made evident that changing charge densities would result in electric fields that would radiate outward

1887 **Heinrich Hertz demonstrated such waves:**

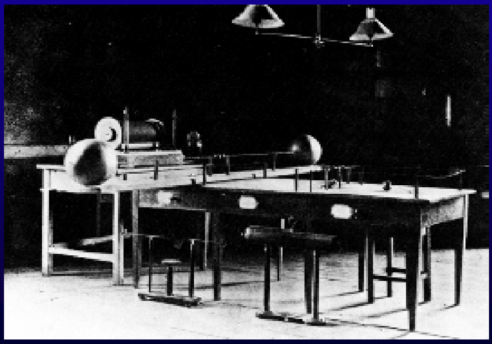

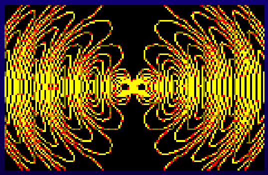

….. this is of no use whatsoever !

Why do they radiate?

Charge at rest: Coulomb field

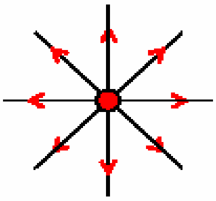

Uniformly moving charge

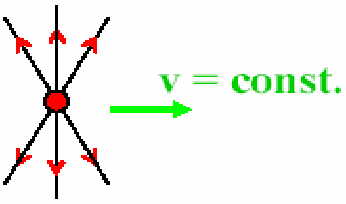

Accelerated charge

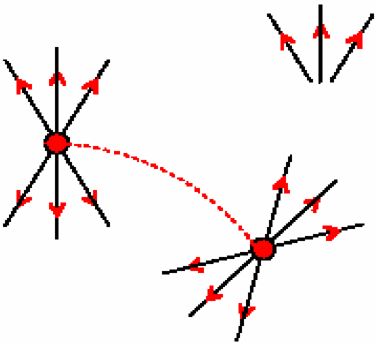

Fields of a moving charge

$$\vec{\mathbf{E}}(t) = \frac{q}{4\pi\varepsilon_0}\left[\frac{\vec{\mathbf{n}}-\vec{\beta}}{\left(1-\vec{\mathbf{n}}\cdot\vec{\beta}\right)^3\gamma^2}\cdot\boxed{\frac{\mathbf{1}}{\mathbf{r}^2}}\right]_{ret} +$$

$$\frac{q}{4\pi\varepsilon_0 c}\left[\frac{\vec{\mathbf{n}}\times\left[\left(\vec{\mathbf{n}}-\vec{\beta}\right)\times\boxed{\dot{\vec{\beta}}}\right]}{\left(1-\vec{\mathbf{n}}\cdot\vec{\beta}\right)^3\gamma^2}\cdot\boxed{\frac{\mathbf{1}}{\mathbf{r}}}\right]_{ret}$$

$$\vec{\mathbf{B}}(t) = \frac{1}{c}\left[\vec{\mathbf{n}}\times\vec{\mathbf{E}}\right]$$

Transverse acceleration

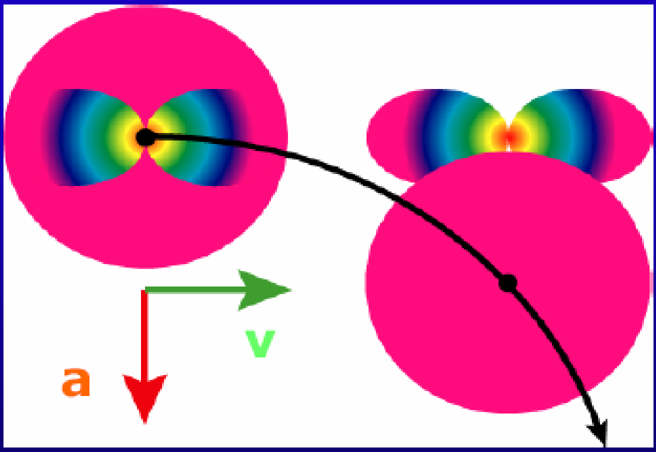

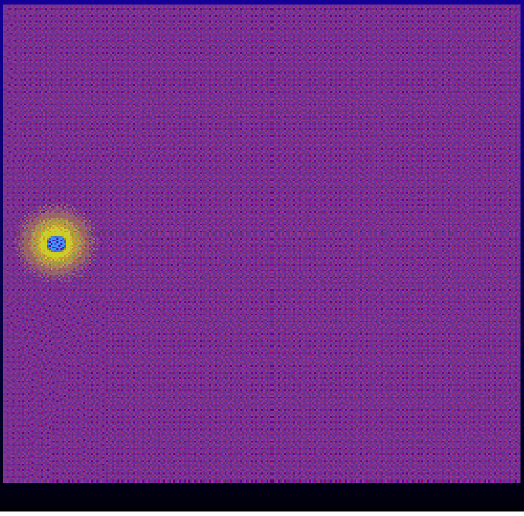

Radiation field quickly separates itself from the Coulomb field

Longitudinal acceleration

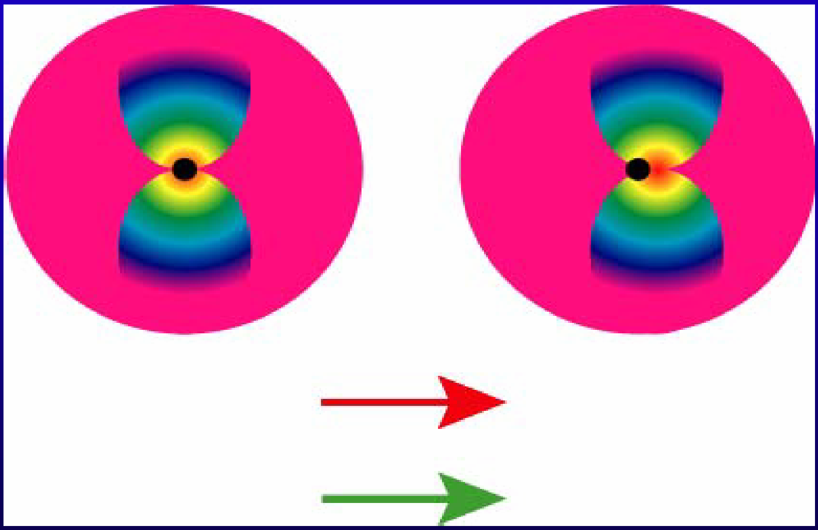

Radiation field cannot separate itself from the Coulomb field

---

Radiation is emitted into a narrow cone

Into a narrow cone

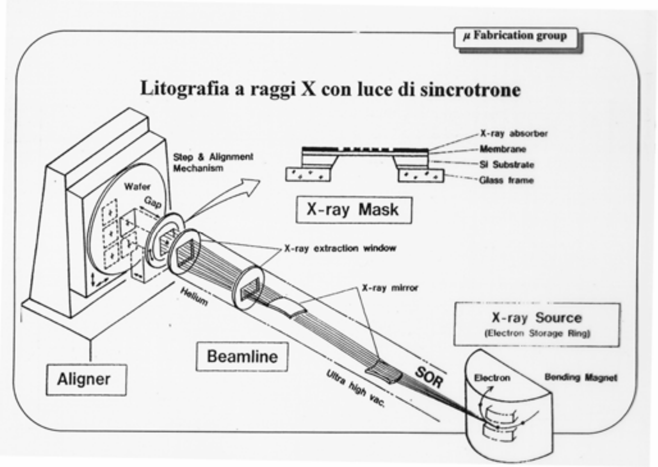

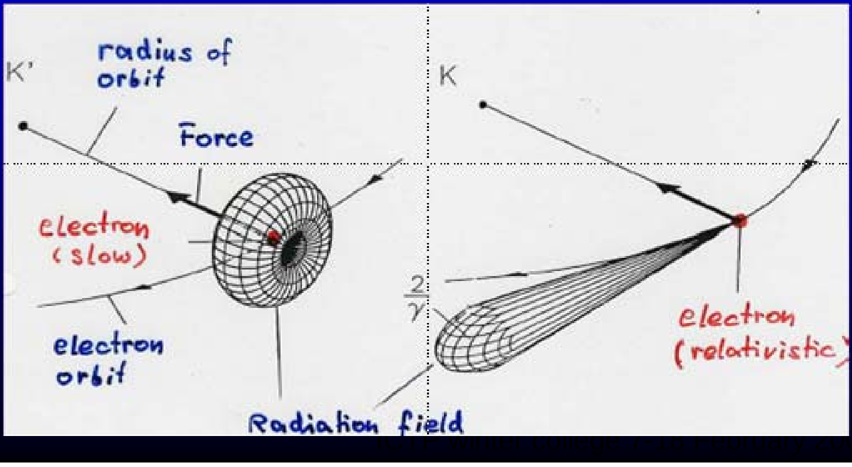

Crab Nebula
6000 light years away

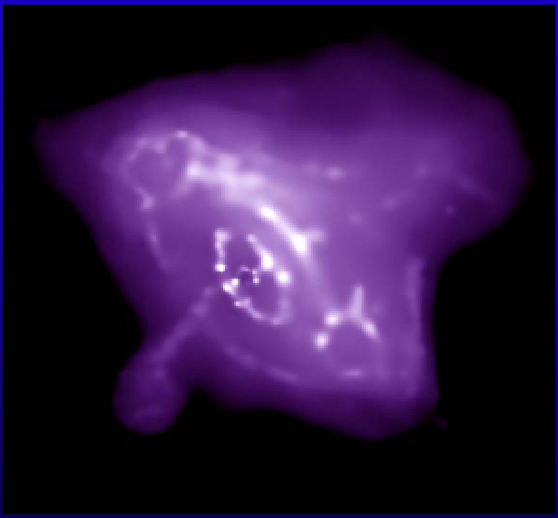

First light observed
1054 AD

GE Synchrotron
New York State

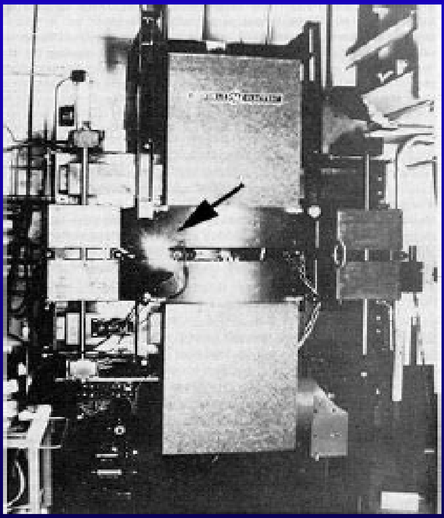

First light observed
1947

---

20 000 users world-wide

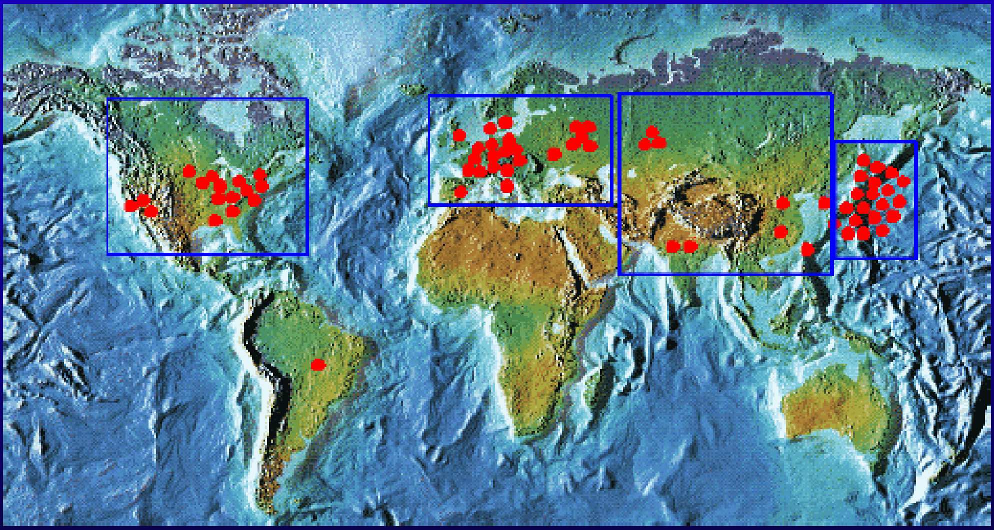

Scheme of a typical synchrotron X-ray lithography system

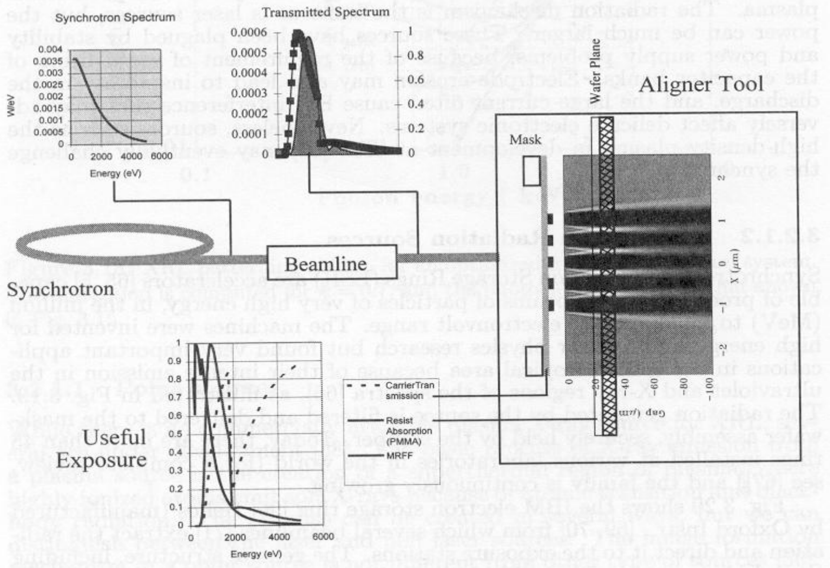

Figure 3.19: Schematic of an X-ray Lithography system based on a synchrotron. Notice the synchrotron, beamline and mask arrangement as well as the changes in the spectrum of the radiation.

Lilit-group

Litografia a raggi X con luce di sincrotrone

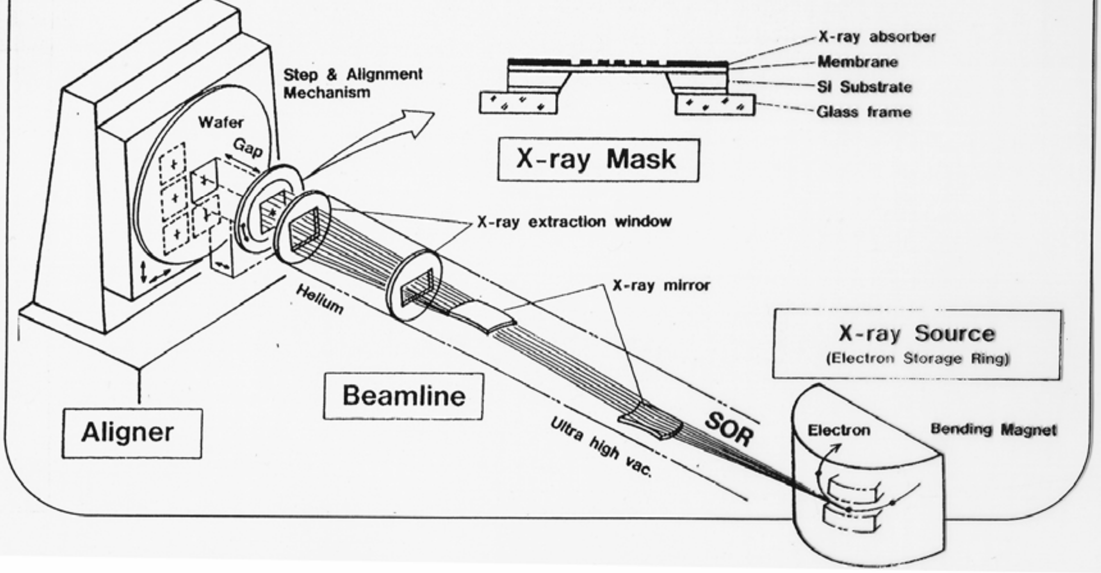

The Stepper

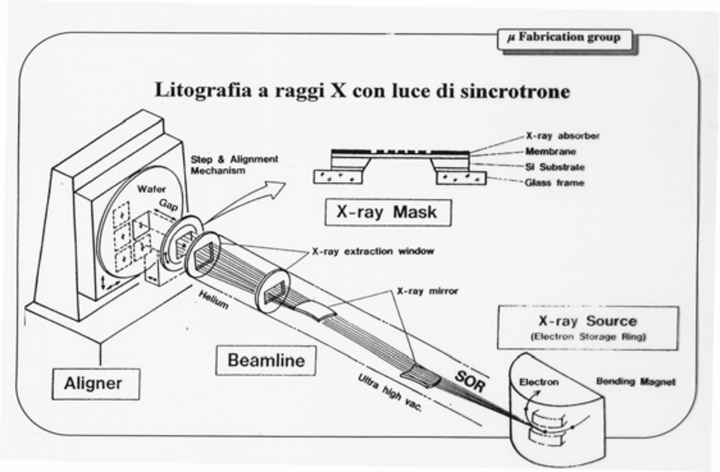

LILIT energy spectrum

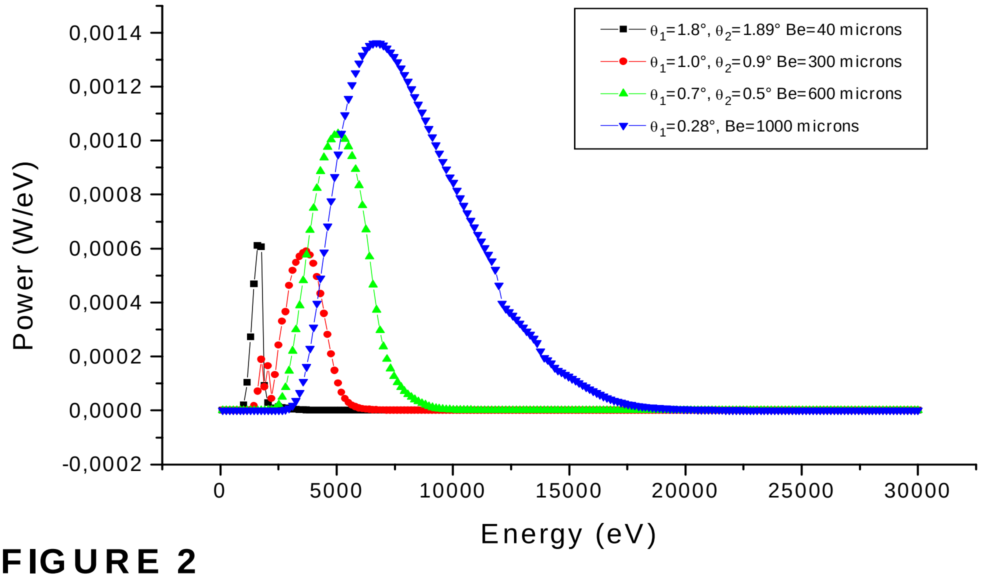

FIGURE 2

Calculated transmission spectra of the beamline for different values of the incidence angles.
The absorption from two Berillium windows of various thicknesses is included in the calculation.

Patterning ability of an X-ray lithography system

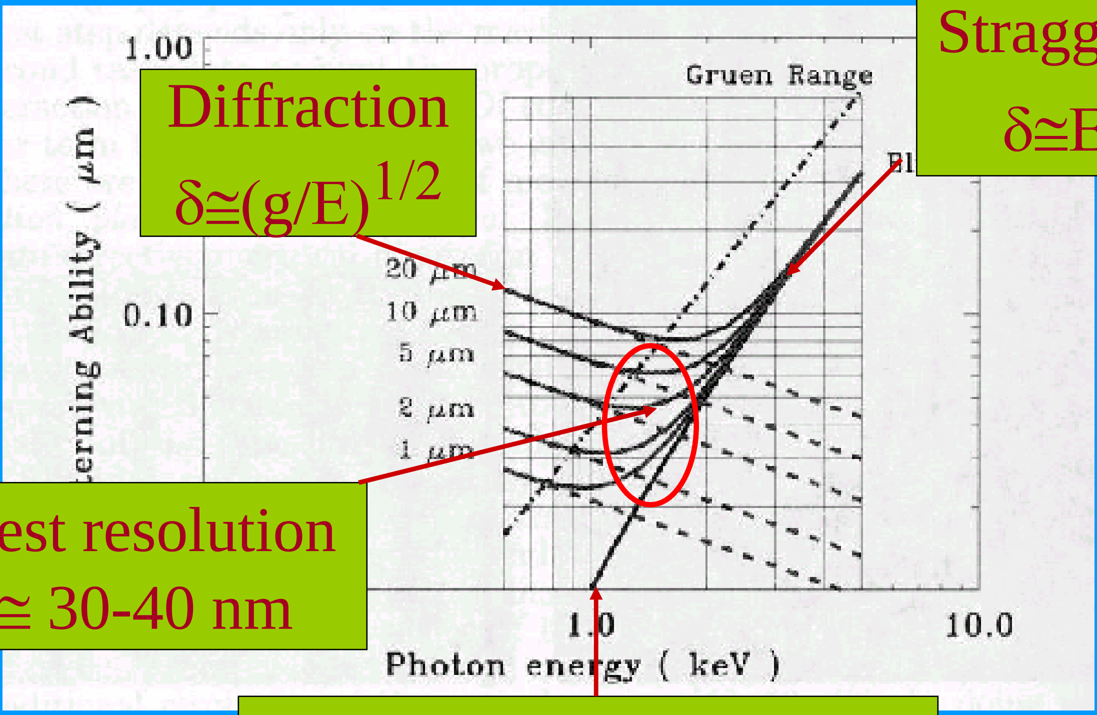

Diffraction
$\delta \cong (g/E)^{1/2}$

Straggling
$\delta \cong E^2$

Best resolution
≅ 30-40 nm

Optimized Energy≅ 1 keV

---

50 nm Test pattern

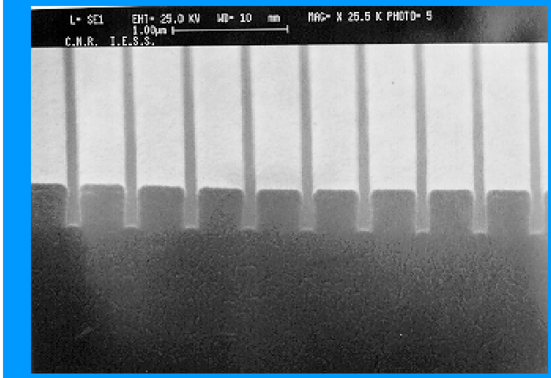

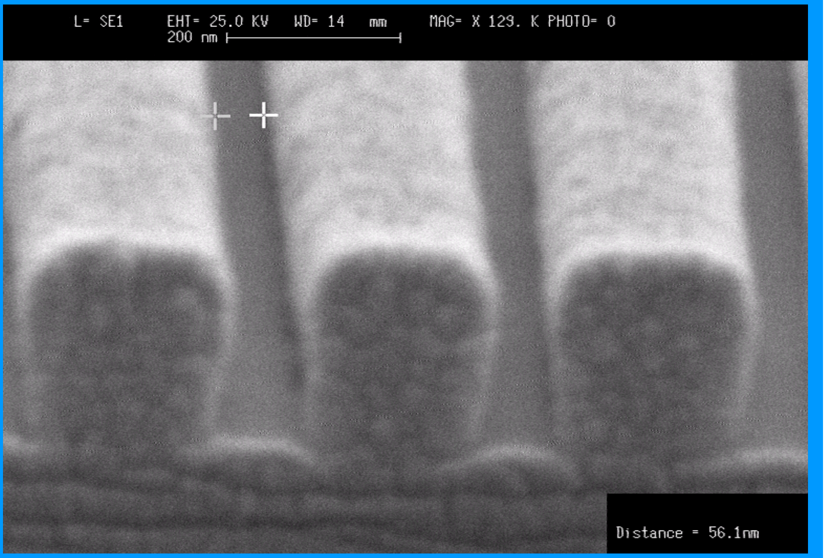

Layered approach for the E.M. field

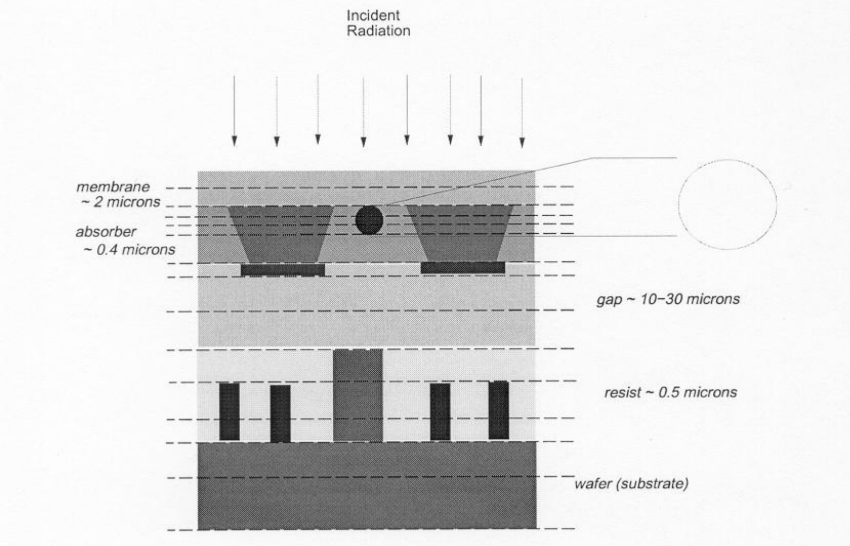

Figure 8: *Illustration of the layered approach. Materials of arbitrary shape can be treated as a stack of layers with varying transmission. The figure is not drawn to scale, in order to show the structure clearly. A spherical particle in the mask can be approximated by circular discs*

Step 1:Compute the transmission of the l-th layer
Step 2:Compute the transmitted E.M. field
Step 3: Obtain the Fourier Tranf. of the E.M.field
Step 4: Propagate the field through the thickness d in the Fourier domain
Step 5:obtain the diffracted E.M. field by inverse FFT
Step 6: go to next layer

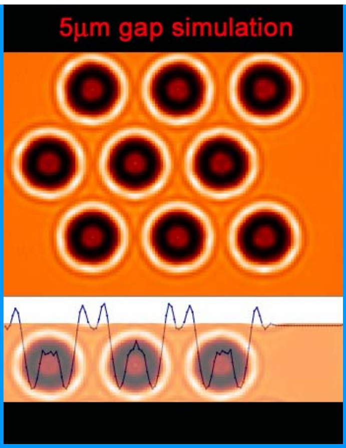
5µm gap simulation

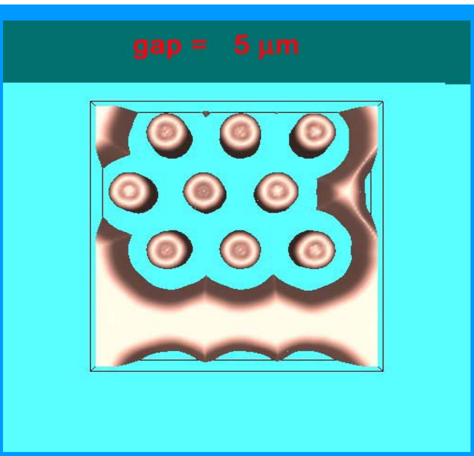
gap = 5 µm

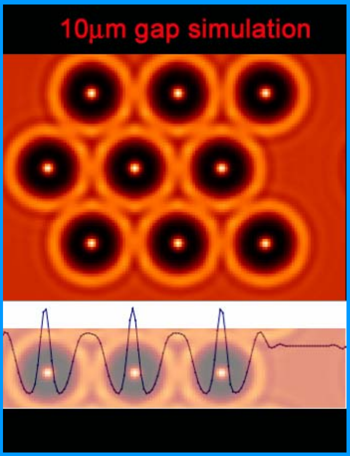
10µm gap simulation

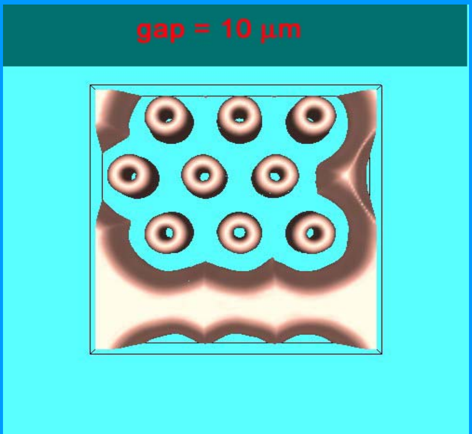
gap = 10 µm

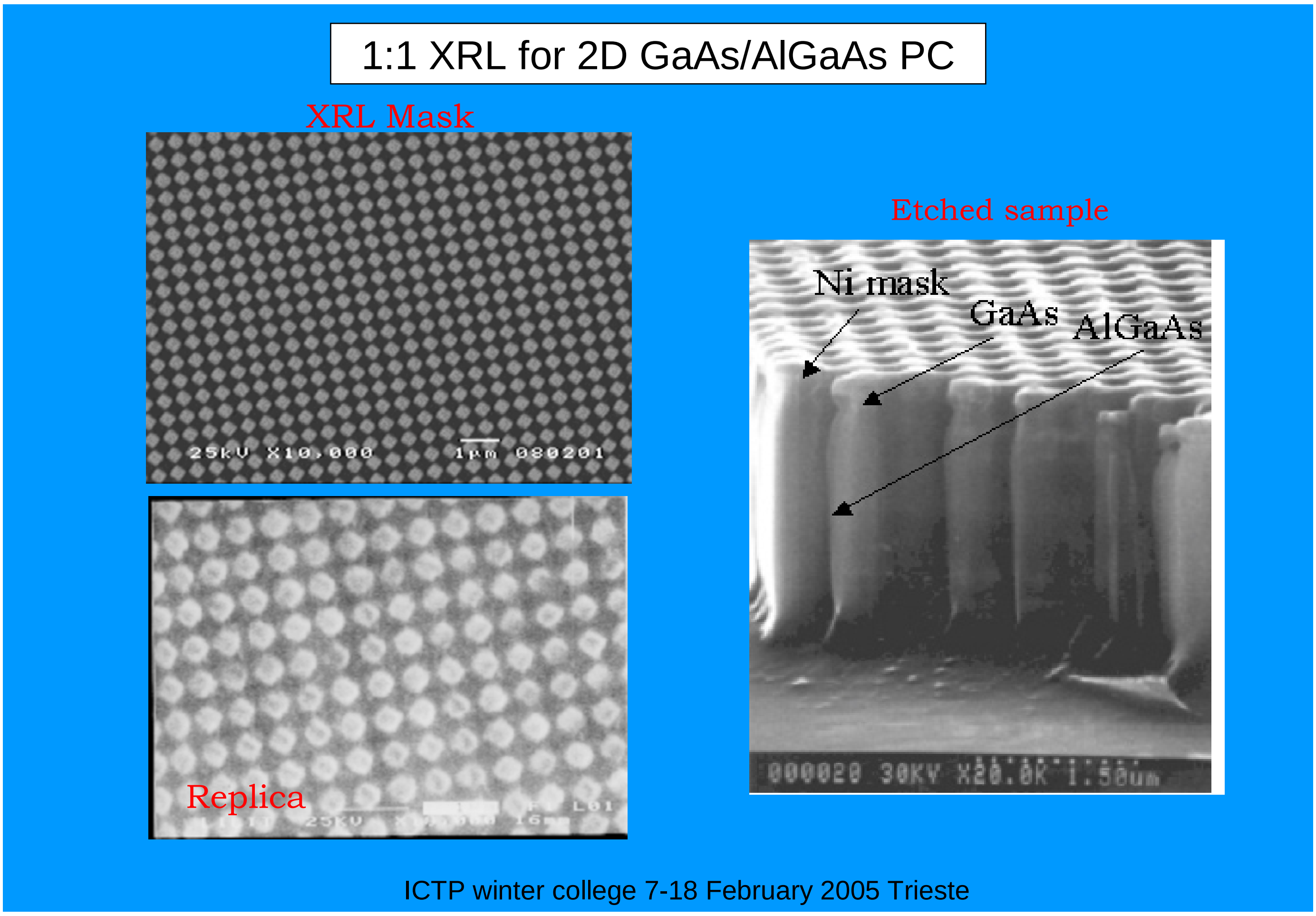

1:1 XRL for 2D GaAs/AlGaAs PC

ICTP winter college 7-18 February 2005 Trieste

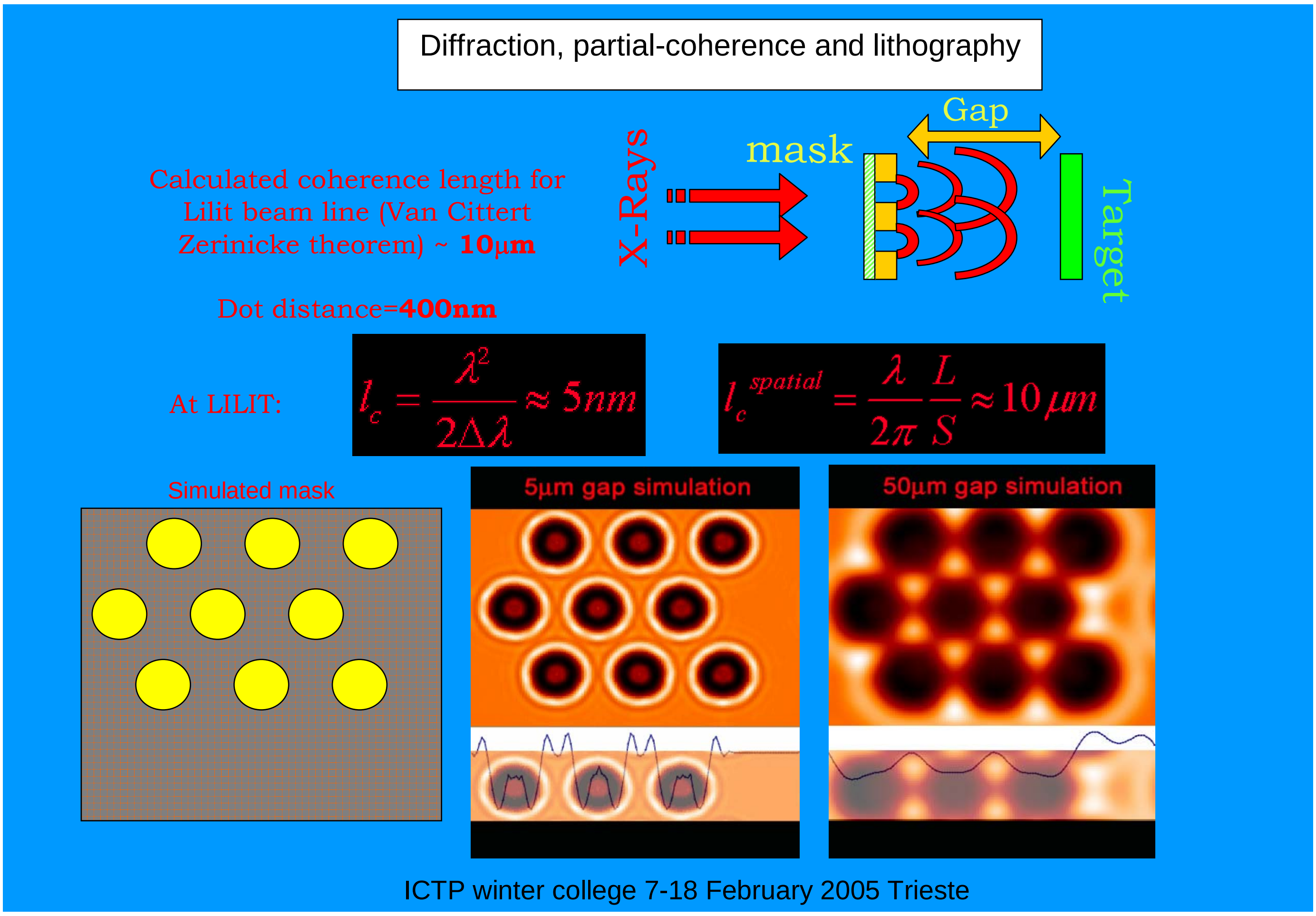

Diffraction, partial-coherence and lithography

Calculated coherence length for Lilit beam line (Van Cittert Zerinicke theorem) ~ **10µm**

Dot distance=**400nm**

At LILIT:

$$l_c = \frac{\lambda^2}{2\Delta\lambda} \approx 5nm$$

$$l_c^{spatial} = \frac{\lambda}{2\pi}\frac{L}{S} \approx 10\,\mu m$$

ICTP winter college 7-18 February 2005 Trieste

Experimental results: unconventional base

XRL Mask

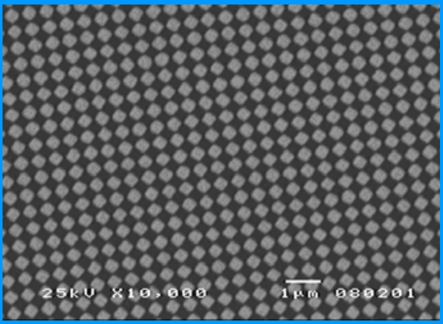

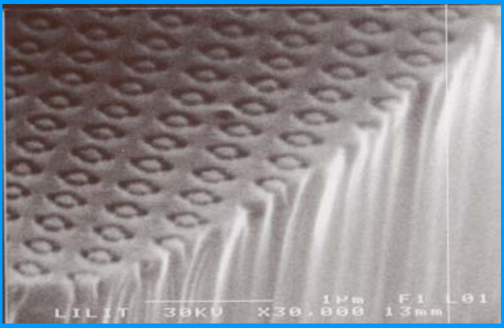

Gap=0µm

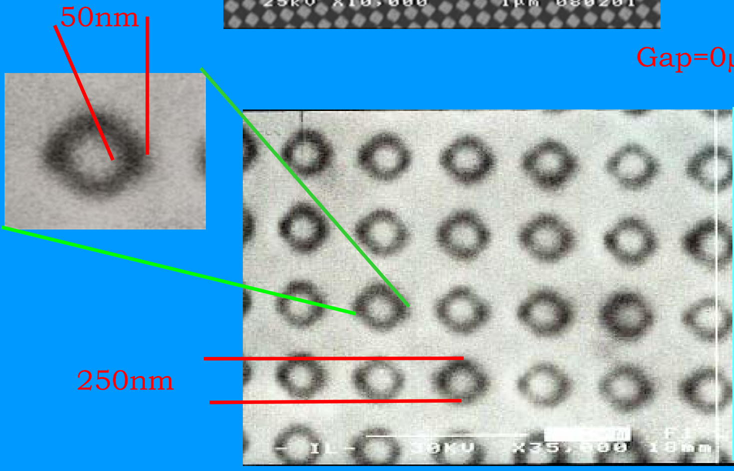

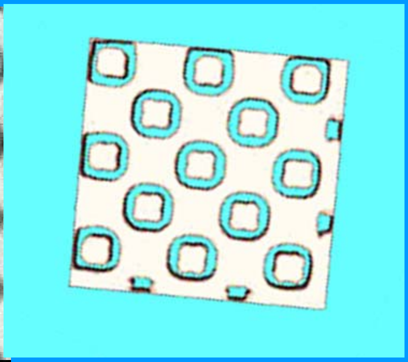

Gap=7µm

INTRODUCTION

Objectives:

- Achievement of 3D resist microstructures in only one shot
- Modulation of the x-ray dose by using a grey tone mask

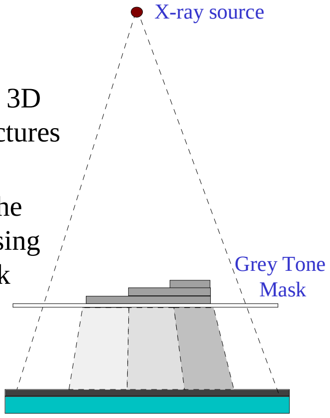

Simulation of illumination effect

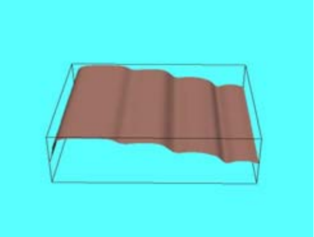

By computer simulation, we obtain this shape for the developed resist exposed by the x-rays passing through the described mask

MASK FABRICATION

Picture of the mask

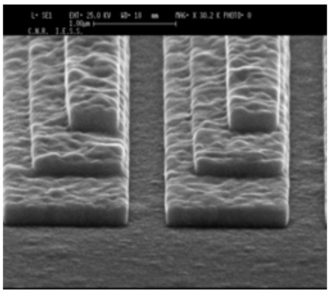

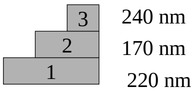

X-RAY EXPOSURES

SEM image of 3D shaped resist

dose of 7000 mJ/cm2, and gap of 13 μm.

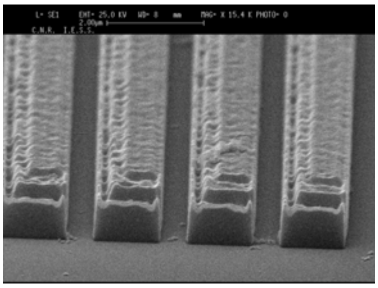

Structures produced with X-ray litho.

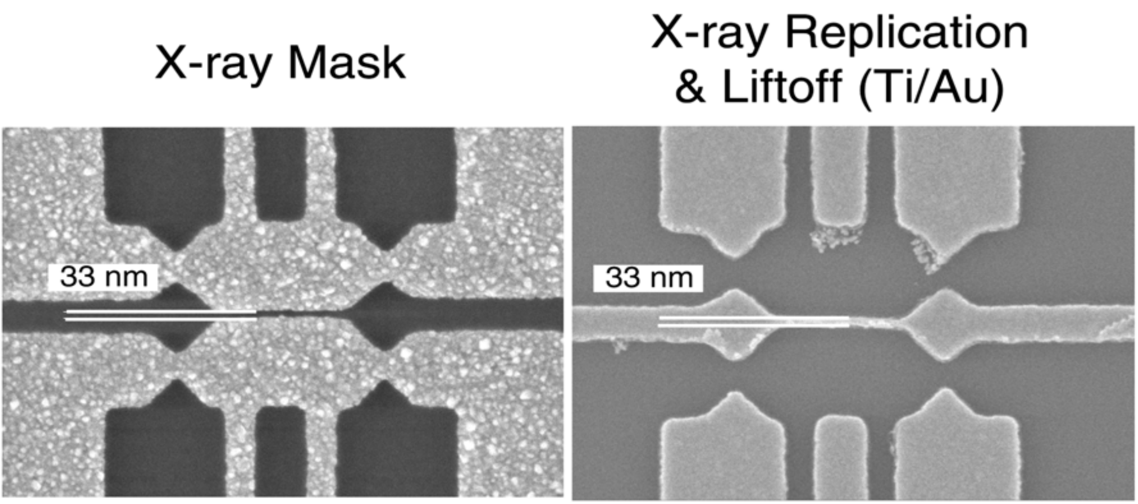

Device patterns with feature sizes less than 40 nm achieved by x-ray lithography and by liftoff.

More ? Check out Prof. H. I. Smith, MIT

Structures produced with X-ray litho. (ctnd.)

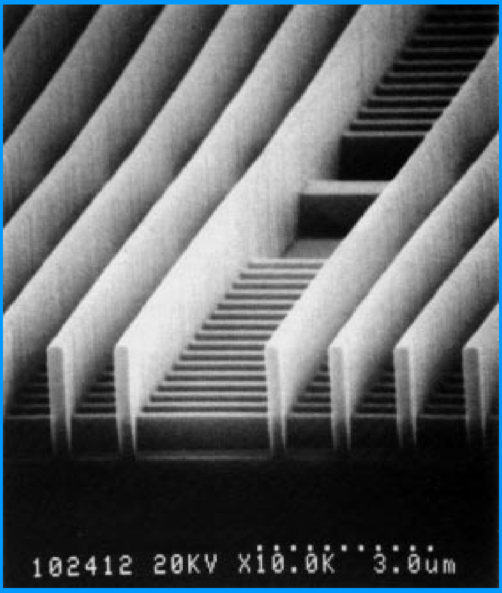

200 nm lines of 2 um thick resist over thick steps (NTT-AT)

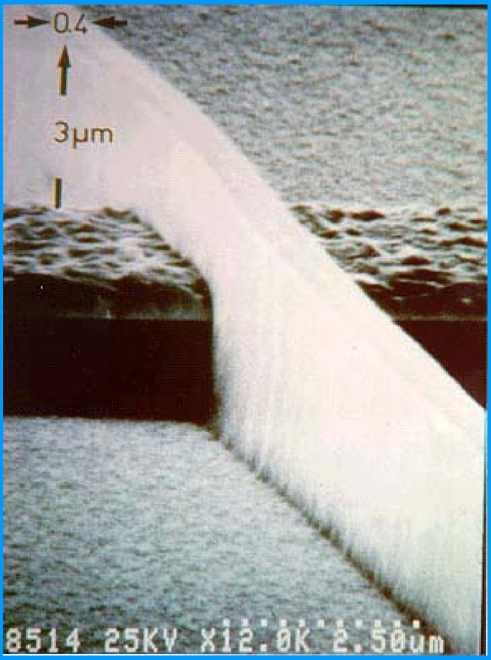

400 nm by 3 um resist over poly line (ISiT)

Source: SAL, Inc.

Electron beam lithography

1) Casting of thin PMMA film

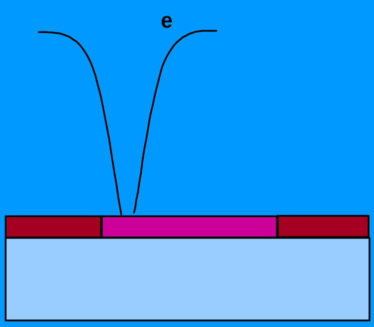

2) E-beam patterning of PMMA

3) Development of PMMA

4) Metallization

5) Lift-off

Employs a beam of electron instead of photons

Advantage: resolution and direct writing method
Disadvantage: Slow throughput

More ? Google it ! **Also, check out R.F.W. Pease, Stanford**

Electron-Beam nanolithography syetsm Installed in Pirelli Labs-Milan

Developed further to the needs of micro-electronics industry, electron-beams are systems able to impress a thin layer of photosensitive material (photoresist) with a resolution orders of magnitude higher than that achieved by optical methods

Typical parameters of operation:

- spot size of the beam: 5nm
- resolution: 15nm (conservative)
- size of the wafer: 8”, 12” standard, larger sizes developed for semiconductor industry

Typical e-beam system used in the production (Leica VB6 HR type)

Electron beam lithography system

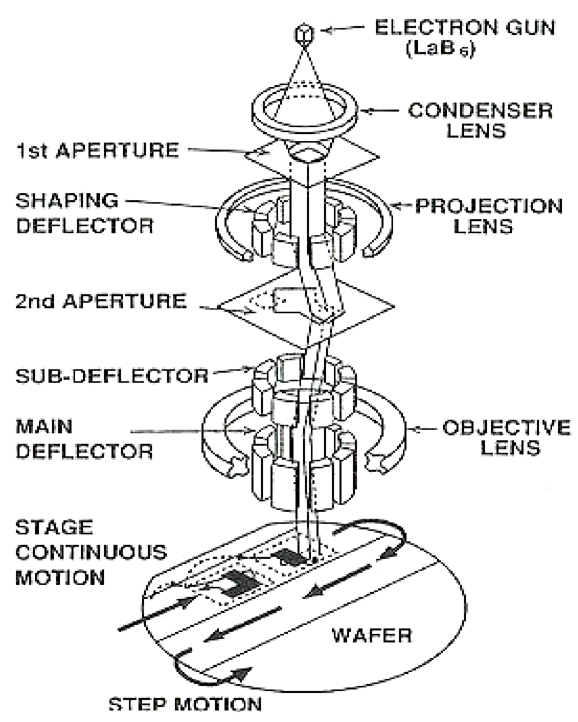

Throughput enhanced by variable beam shaping

Effects produced by electron bombardment of a material.

Two major factors control which effects can be detected from the interaction volume. First, some effects are not produced from certain parts of the interaction volume (Figure 2.1b).
Beam electrons lose energy as they traverse the sample due to interactions with it and if too much energy is required to produce an effect, it will not be possible to produce it from deeper portions of the volume. Second, the degree to which an effect, once produced, can be observed is controlled by how strongly it is diminished by absorption and scattering in the sample.
For example, although secondary and Auger electrons are produced throughout the interaction volume, they have very low energies and can only escape from a thin layer near the sample's surface. Similarly, soft X-rays, which are absorbed more easily than hard X-rays, will escape more readily from the upper portions of the interaction volume. Absorption is an important phenomenon and is discussed in more detail below.

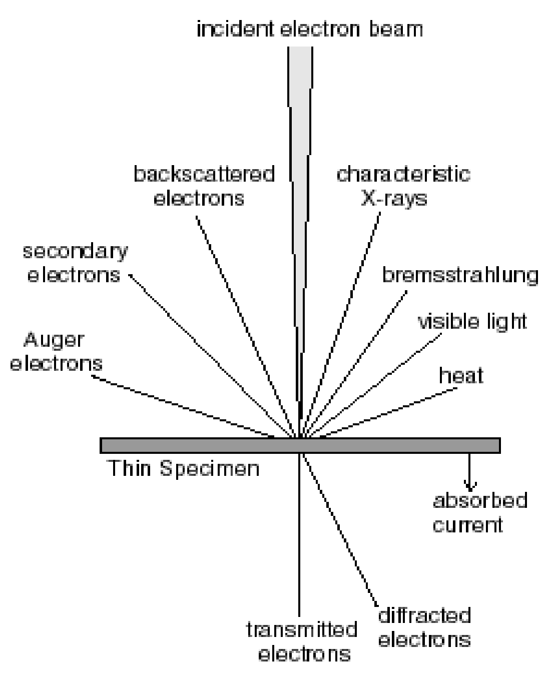

Interaction volumes

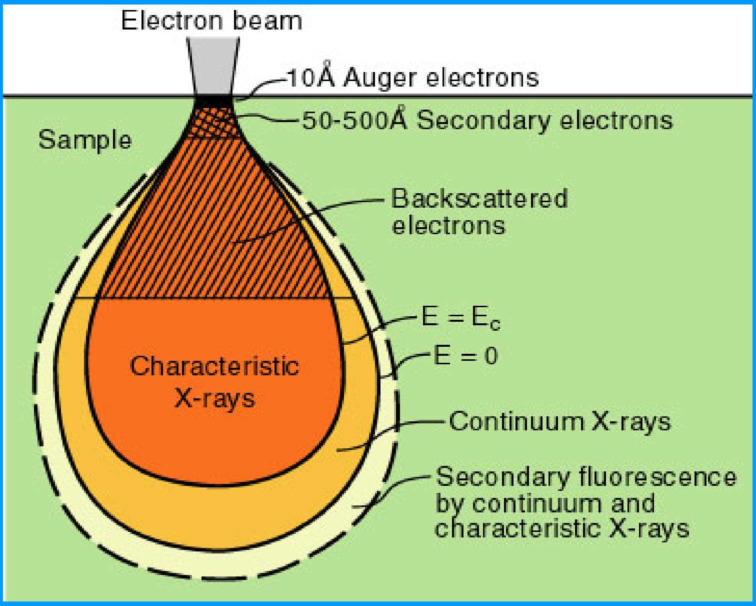

Figure 2.1b. Generalized illustration of interaction volumes for various electron-specimen interactions. Auger electrons (not shown) emerge from a very thin region of the sample surface (maximum depth about 50 Å) than do secondary electrons (50-500 Å).

Volume of Excitation

Two factors limit the size and shape of the interaction volume: (1) energy loss through inelastic interactions and (2) electron loss or backscattering through elastic interactions. The resulting excitation volume is a hemispherical to jug-shaped region with the neck of jug at the specimen surface. The analyst must remember that the interaction volume penetrates a significant depth into the sample and avoid edges where it may penetrate overlapping materials. The depth of electron penetration of an electron beam and the volume of sample with which it interacts are a function of its angle of incidence, the magnitude of its current, the accelerating voltage, and the average atomic number (Z) of the sample. Of these, accelerating voltage and density play the largest roles in determining the depth of electron interaction (Figure 2.2a).

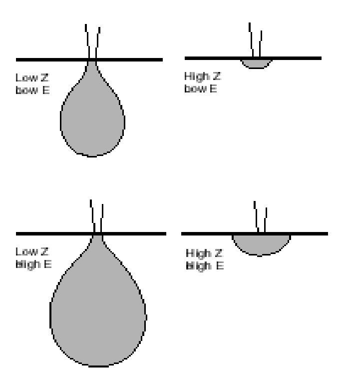

Figure 2.2a. Schematic depiction of the variation of interaction volume shape with average sample atomic number (Z) and electron beam accelerating voltage (E_o). The actual shape of the interaction volume is not as long-necked since the electron beam in microprobe analysis has a diameter of about 1 µm (see Figure 2.1b).

$$x\ (\mu m) = \frac{0.1\ E_o^{1.5}}{\rho}$$

where E_o = accelerating voltage (keV),
and ρ = density (g/cm^3)

Electron penetration generally ranges from 1-5 µm with the beam incident perpendicular to the sample. The depth of electron penetration is approximately (Potts, 1987, p. 336):

For example, bombarding a material with a density of 2.5 g/cm3, about the minimum density for silicate minerals, with E_o = 15 keV, gives x = 2.3 µm. The width of the excited volume can be approximated by (Potts, 1987, p. 337):

Both of these are empirical expressions. A theoretical expression for the "range" of an electron, the straight line distance between where an electron enters and its final resting place, for a given E_o is (Kanaya & Okayama, 1972):

The volume of interaction can be modeled by Monte Carlo simulation. In such models, the likelihood of incident electrons interacting with the sample and scattering and the angle of deflection are determined probabilistically. X-ray generation depths depend strongly on density and accelerating voltage (Figure 2.2b.). The results derived from Monte Carlo modeling yield a volume of interaction that is very similar to that determined by etching experiments. The excited volume is roughly spherical and truncated by the specimen surface. The depth of the center of the sphere decreases with increasing atomic number of the target.

$$y\ (\mu m) = \frac{0.077\ E_o^{1.5}}{\rho}$$

where E_o = accelerating voltage (keV),
and ρ = density (g/cm^3)

$$r\ (\mu m) = \frac{2.76 \times 10^{-2}\ A\ E_o^{1.67}}{\rho\ Z^{0.89}}$$

where ρ = density of the material (g/cm^3),
Z = atomic number,
A = atomic mass,
and E_o = accelerating voltage.

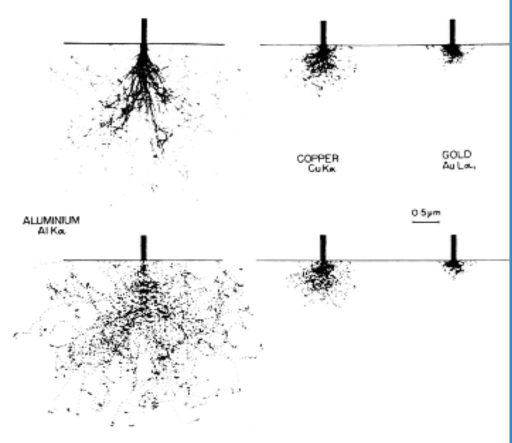

Figure 2.2b. Comparison of electron paths (top) and sites of X-ray excitation (bottom) in targets of aluminum, copper, and gold at 20 keV, simulated in a Monte Carlo procedure (after Heinrich, 1981).

PEC(Proximity Effect Correction)
a. Dose Distribution due to PE

G (x) EID (Exposure Intensity Distribution)function

(Dose distribution of EB resist at one point (x=0) irradiation)

$$g(\boldsymbol{x}) = \mathrm{C}\{g_f(\boldsymbol{x}) + \eta_E g_b(\boldsymbol{x})\}, \qquad (1)$$

$$g_f(\boldsymbol{x}) = (1/\pi\sigma_f^2)\,exp\{-(\boldsymbol{x}-\boldsymbol{x}')^2/\sigma_f^2\} \qquad (2)$$

$$g_b(\boldsymbol{x}) = (1/\pi\sigma_b^2)\,exp\{-(\boldsymbol{x}-\boldsymbol{x}')^2/\sigma_b^2\} \qquad (3)$$

(Parameter)

gf (x):	**Term for forward scattering electron (FSE)**
gb (x):	**Term for backward scattering electron (BSE)**
ηE:	**gf (x)/gb (x)**
σ f f:	**Forward scattering coefficient**
:	**Backward scattering coefficient**
C:	**Constant**

(Factor for parameter)

1. **Material of substrate**
2. **Acceleration voltage**
3. **Resist material**
4. **Resist thickness**

EBL - Electron-Solid interaction

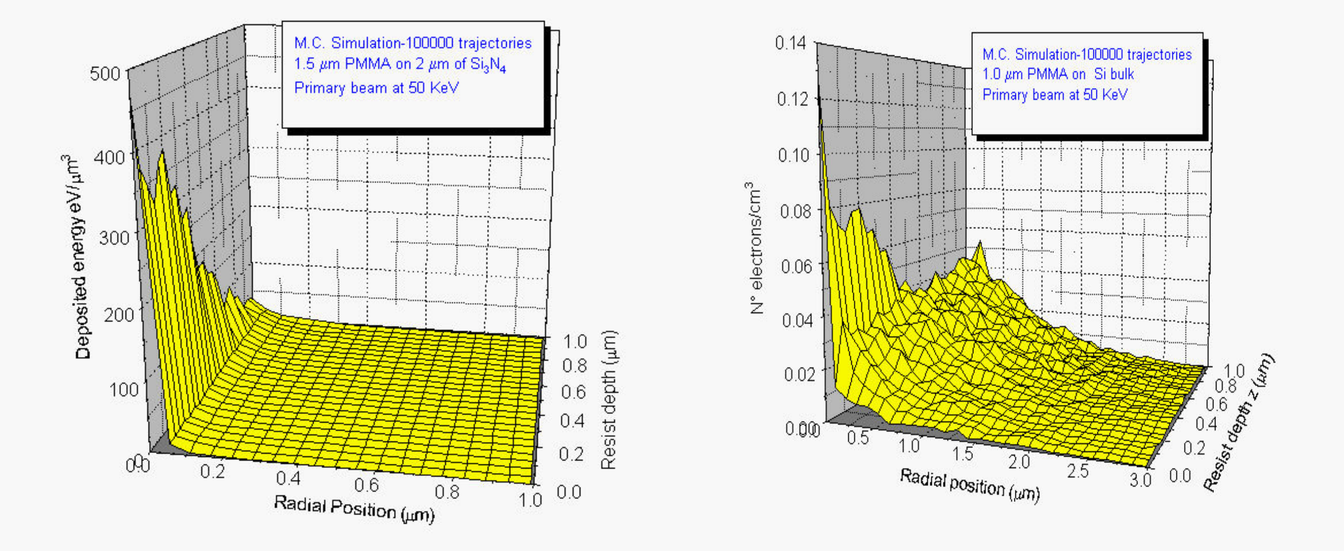

$$\mathrm{I} = \mathbf{A}\mathrm{D} \qquad a_{ij} \propto \int_{A_i}\int_{A_j} f(r_{ij})\,dA_i\,dA_j$$

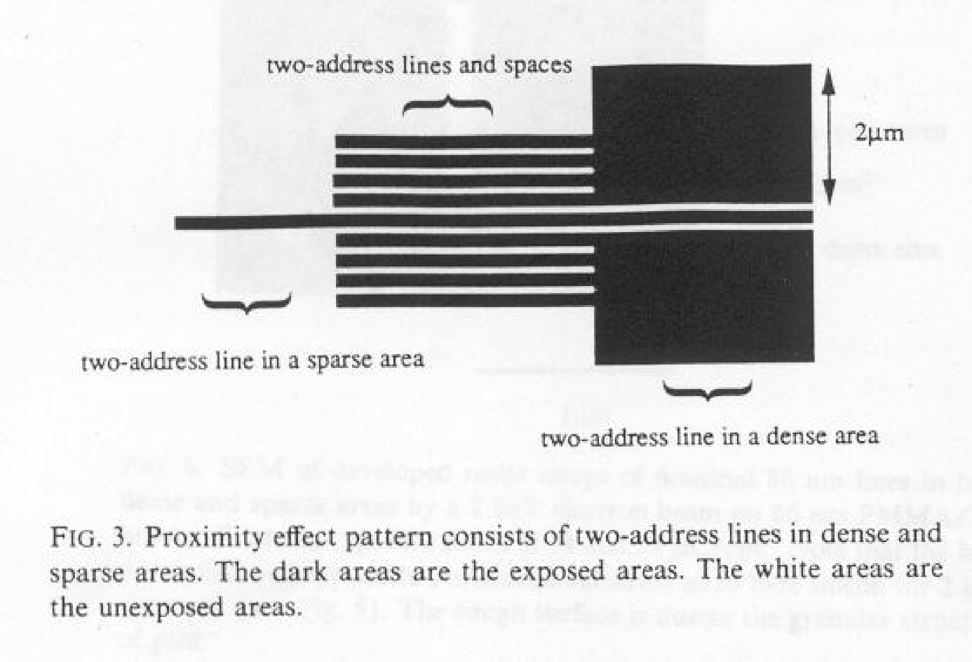

FIG. 3. Proximity effect pattern consists of two-address lines in dense and sparse areas. The dark areas are the exposed areas. The white areas are the unexposed areas.

Cause of Proximity Effect

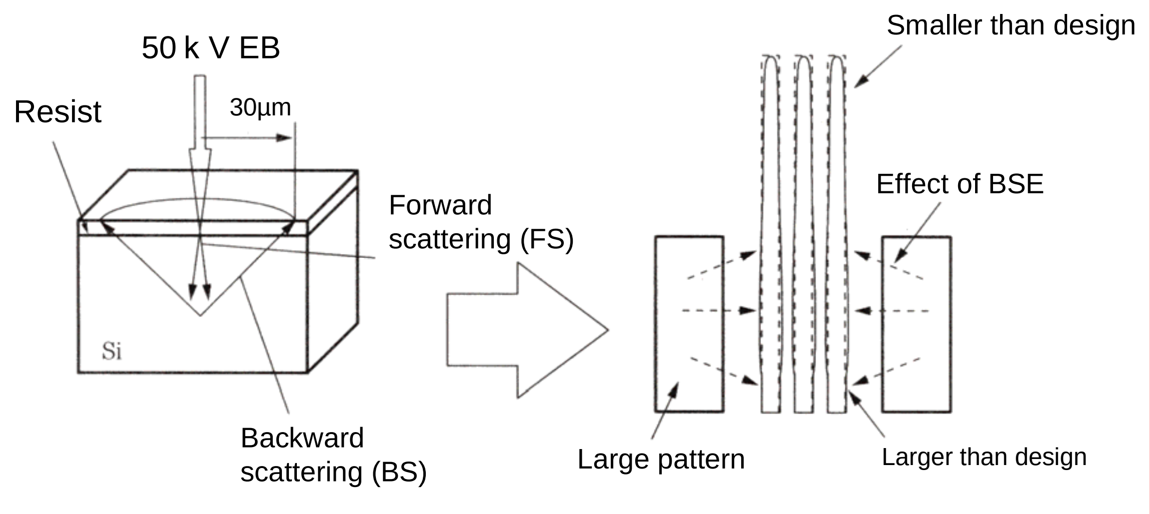

(a) (b)

(a) Electron scattering (b) Pattern size change caused by BSE from peripheral patterns

Simulation for Incident Electron trajectories

Vacc:50kV， Substrate: Si Wafer， Resist Thickness：300nm

Resist + Substrate | **Resist Part Enlargement**

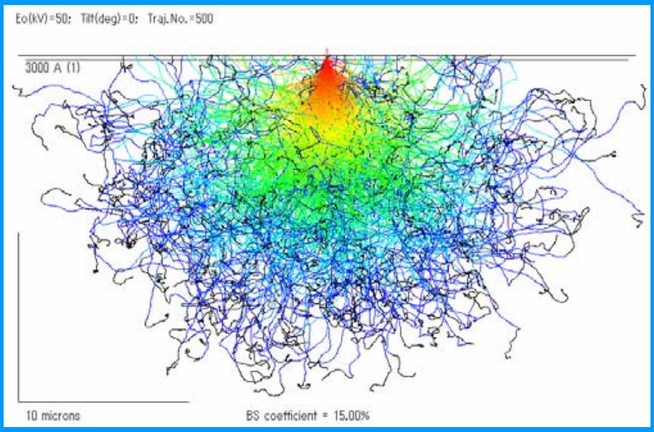

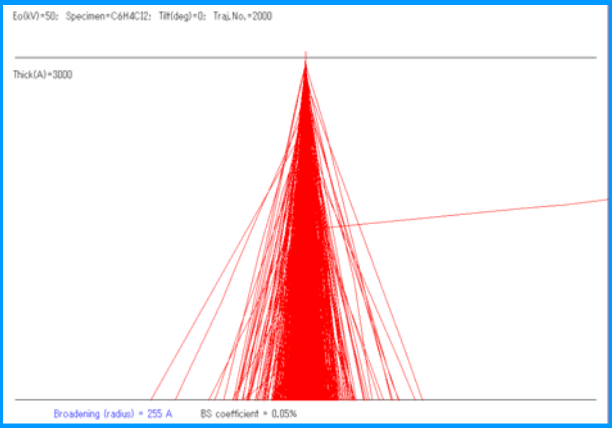

Simulation for Incident Electron trajectory

Vacc:30kV， Substrate:Si Wafer， Resist Thickness：300nm

Resist + Substrate | **Resist Part Enlargement**

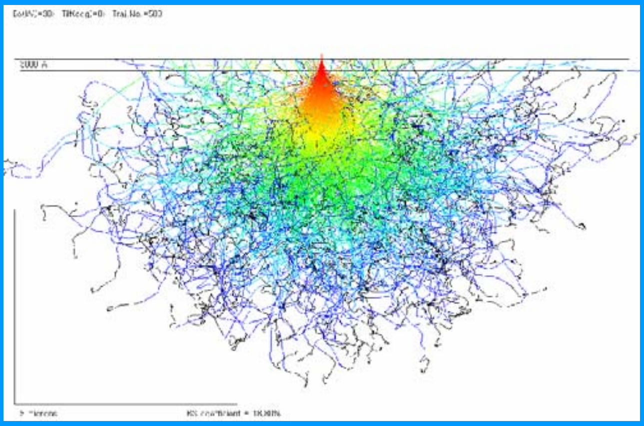

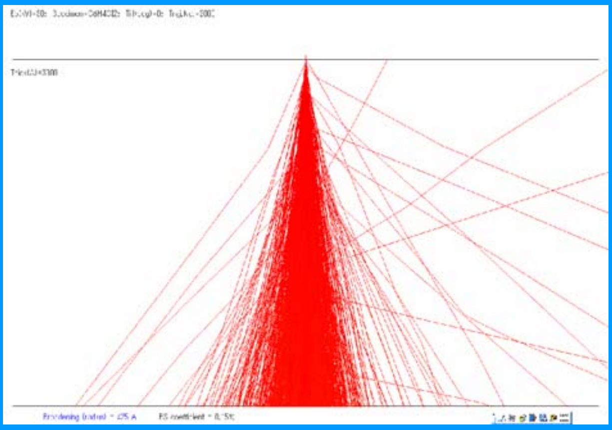

Dose Distribution (DD) Simulation

* Resist dose amount at X in case of irradiating pattern A

$$\boxed{\begin{array}{l} E(x)=\int D(x')g(x-x')dx' \\ X \ni A \end{array}}$$

When,

Integration: area A irradiated by EB

D(x´): Irradiation amount at x ´

* Pattern dependence of resist dose amount

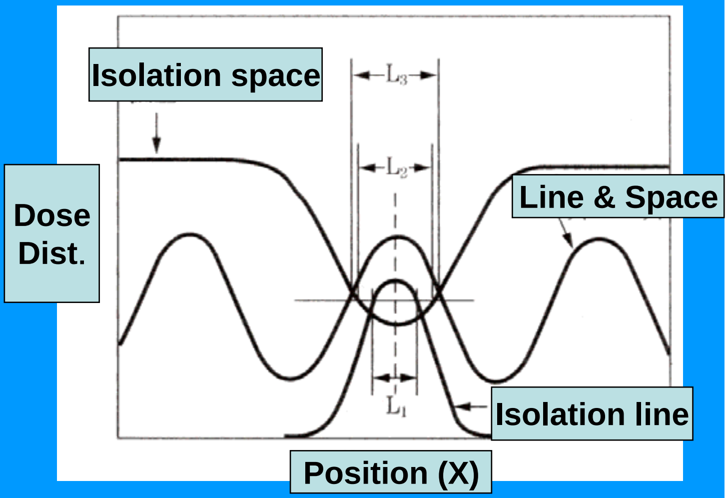

Dose distribution changes due to pattern density.

Dose Distribution (DD) Simulation (2)

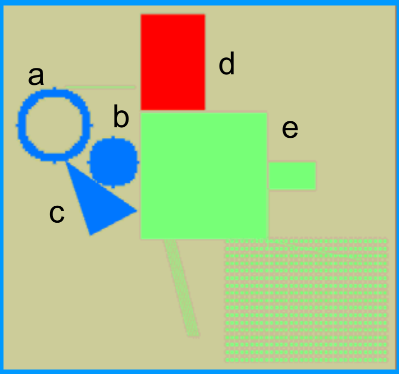

🟥 : E B uniform irradiation

🟩 : E B uniform irradiation

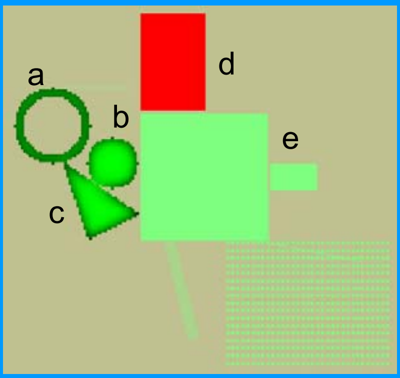

DD of a,b,c change due to EB irradiation at d.

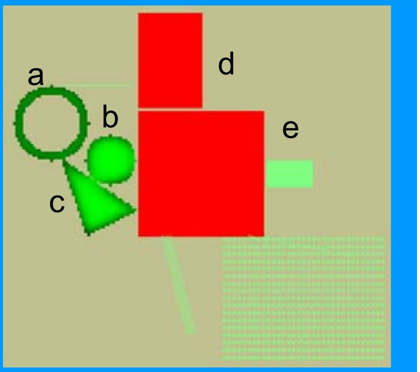

DD of a,b,c change again due to EB irradiation at e.

Dose Distribution Simulation vs Writing Result

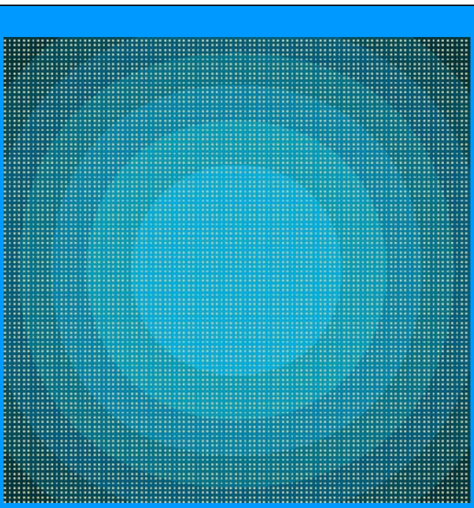

(Simulation parameter)

Backward scattering coeffi. : 3µm

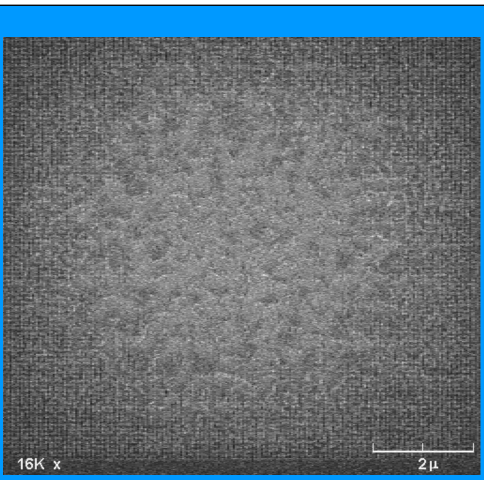

(Writing cond)

Vacc : 30kv,	Field size : 500µm□
Dose Time :	6.25µsec/dot × 0.6
Pattern : 50 nm L&S lattice	
	(Double exposures at cross points)
Writing area :	10µm□, Resist : ZEP520
Resist thickness :	300nm

Main PEC Methods

1. Irradiation Correction:	**To adjust irradiation amount every position**
2. Ghost :	**To suppress dose amount change by carrying out additional irradiation**
3. Pattern Shape Correction:	**To change in advance pattern size in view of affect of peripheral patterns**

Proximity Effect for 100nm L&S Lattice

45% Nominal dose

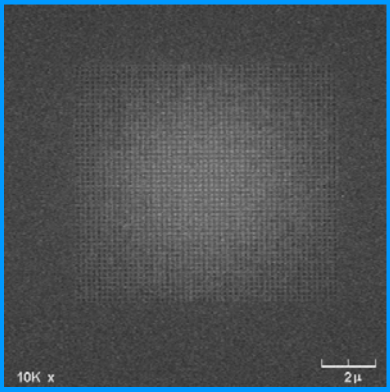

50% Nominal dose

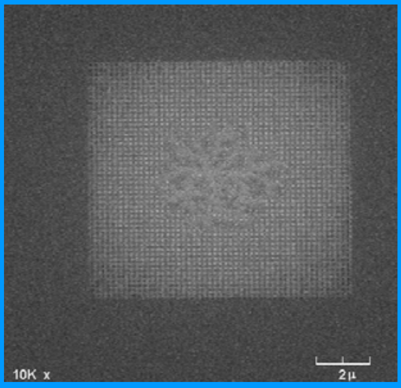

55%% Nominal

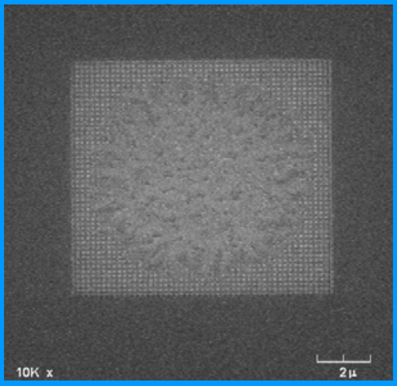

(Writing conditions)

Vacc:	**30kV**	**Nominal Dose:**	**50μC/cm^2(6.25μsec/dot)**
Field Size:	**500μm**	**Resist:**	**ZEP520**
Writing Area:	**10μm**	**Resist Thickness:**	**300nm**
Cross Point:	**Double exposure**		

PEC(Proximity Effect Correction) for 100nm L&S Lattice

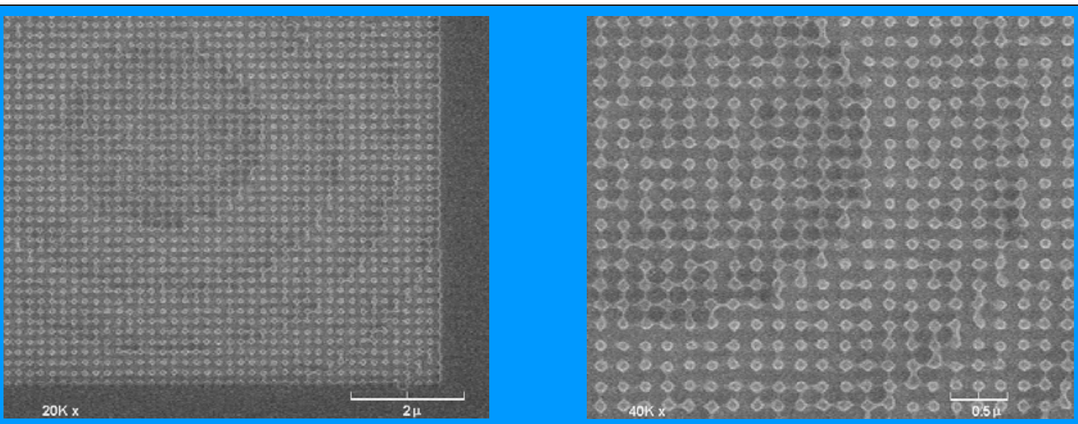

(Writing Conditions)

Vacc:	**30kV**
Field Size:	**500μm**
Writing Area:	**10 μm**
Resist / Thickness:	**ZEP520/300nm**
Pixel:	**20,000 x 20,000 dot**
I B:	**50pA**

(PEC Conditions)

PEC:	**Irradiation amount correction**
Correction Amount:	**5 stage corr. as base of nominal dose on basis of simulation result**
Nominal Dose:	**50μC/cm^2 (6.25μsec/dot)**

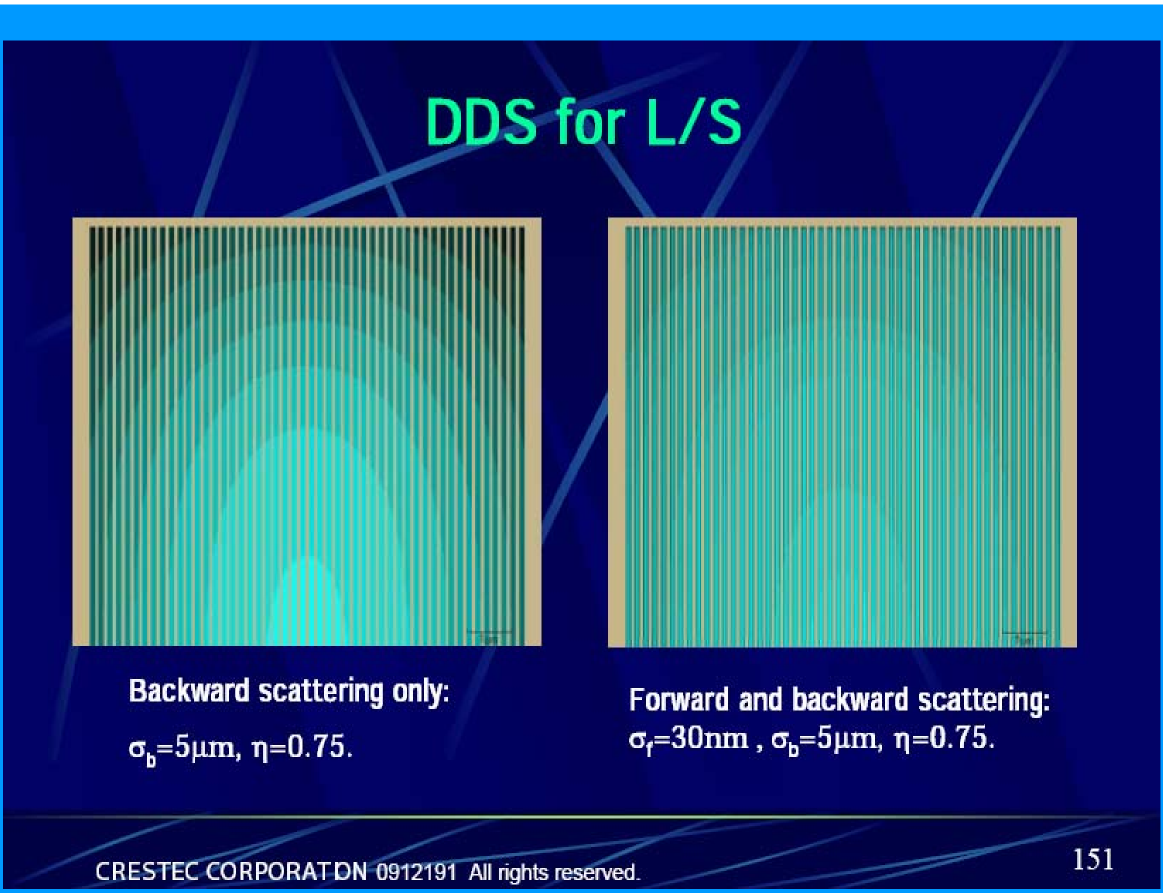

DDS for L/S

Backward scattering only:

σ_b=5μm, η=0.75.

Forward and backward scattering:

σ_f=30nm , σ_b=5μm, η=0.75.

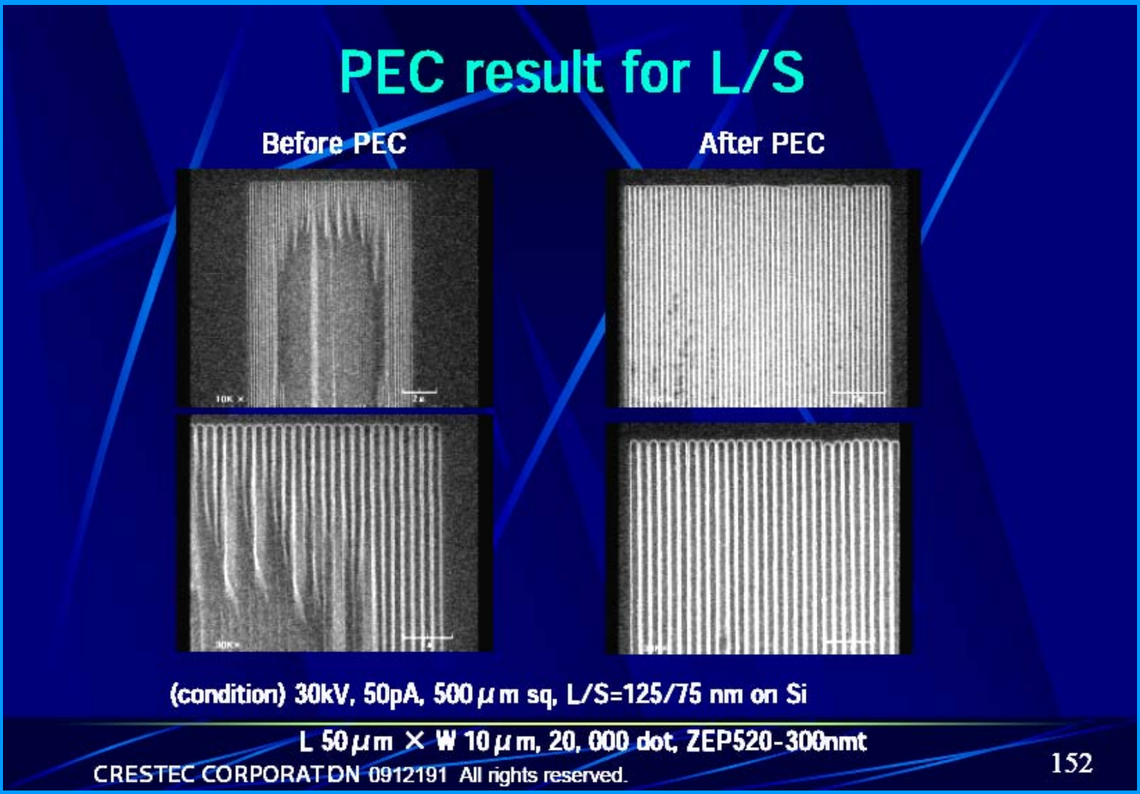

PEC result for L/S

Before PEC **After PEC**

(condition) 30kV, 50pA, 500 μm sq, L/S=125/75 nm on Si

L 50 μm × W 10 μm, 20, 000 dot, ZEP520-300nmt

Resist Thickness Dependence of Proximity Effect

Resist Thickness: 50nm **:100nm** **:500nm**

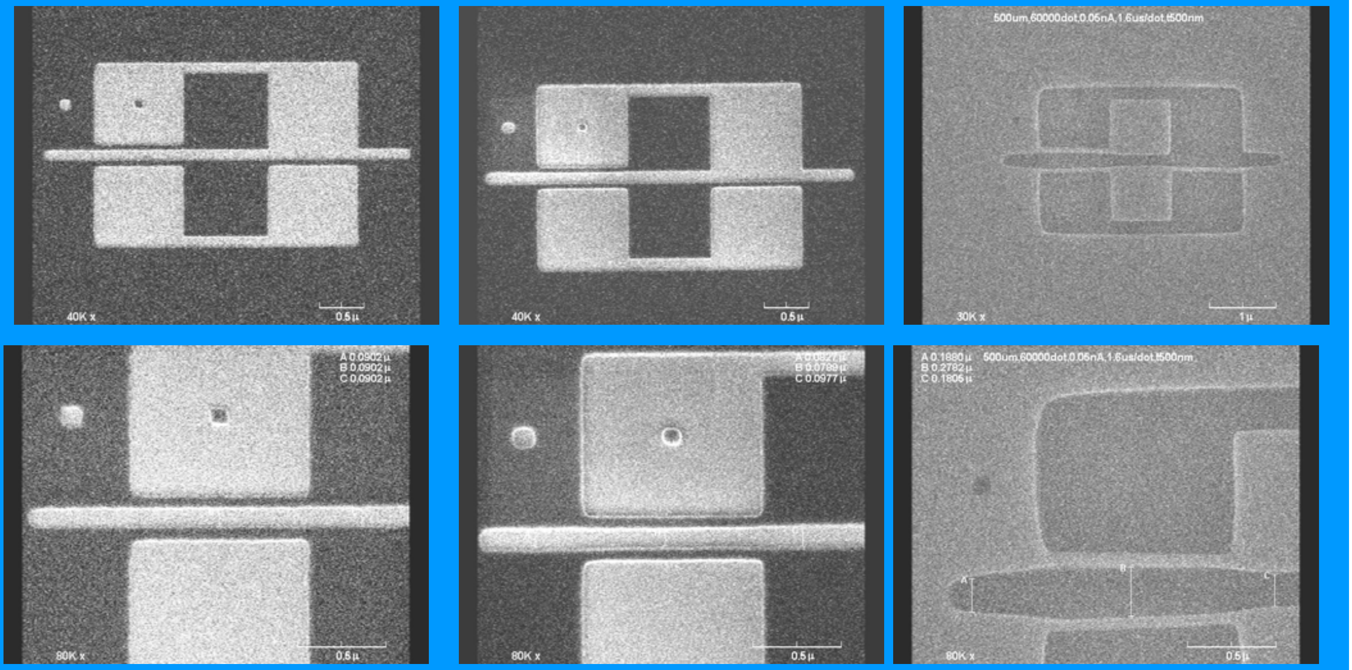

Without PE Correction

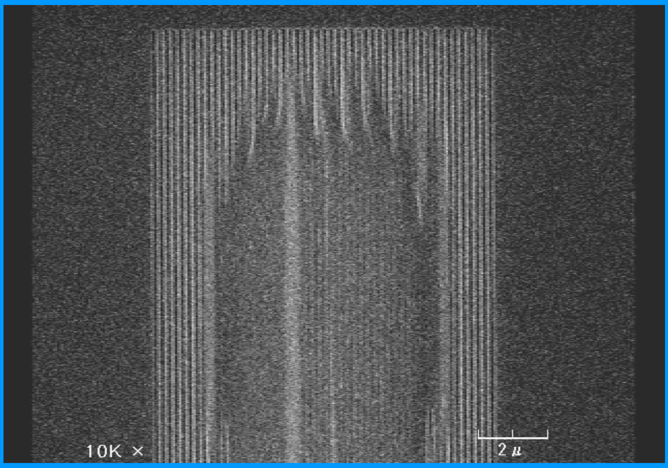

ZEP520 300nm thickness on Si sub.

e^- Beam = 30kV / 50pA

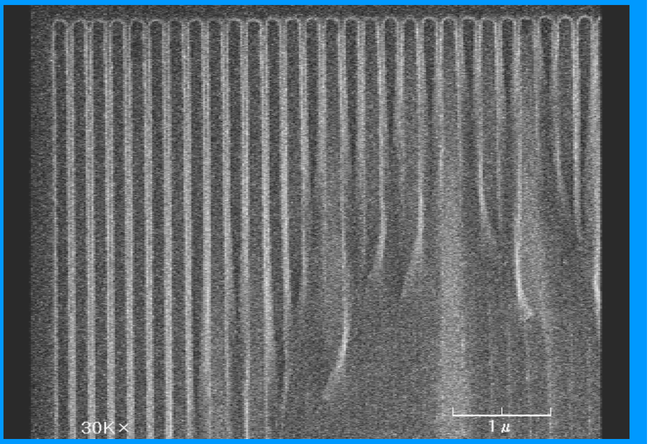

Pattern design:
500mm field, 20000dot
=Line 125nm/Space 75nm
Size: 50mm x10mm

With PEC Correction

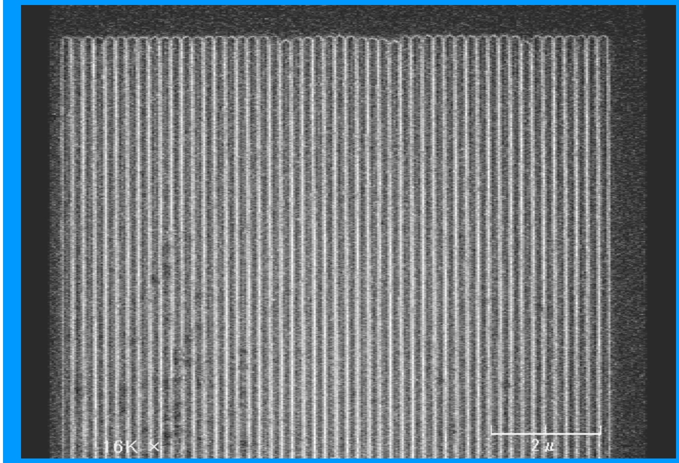

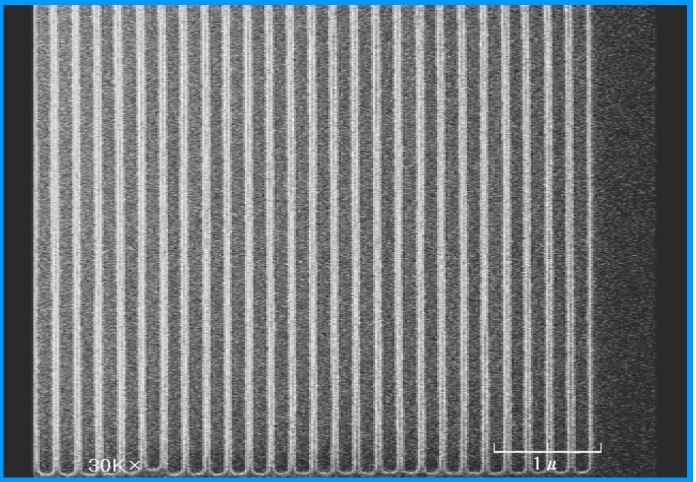

Collection point 2, connection 2/3,
quantization level 6

Proximity Effect Correction

(Data supplied by Thales Research & Technology)

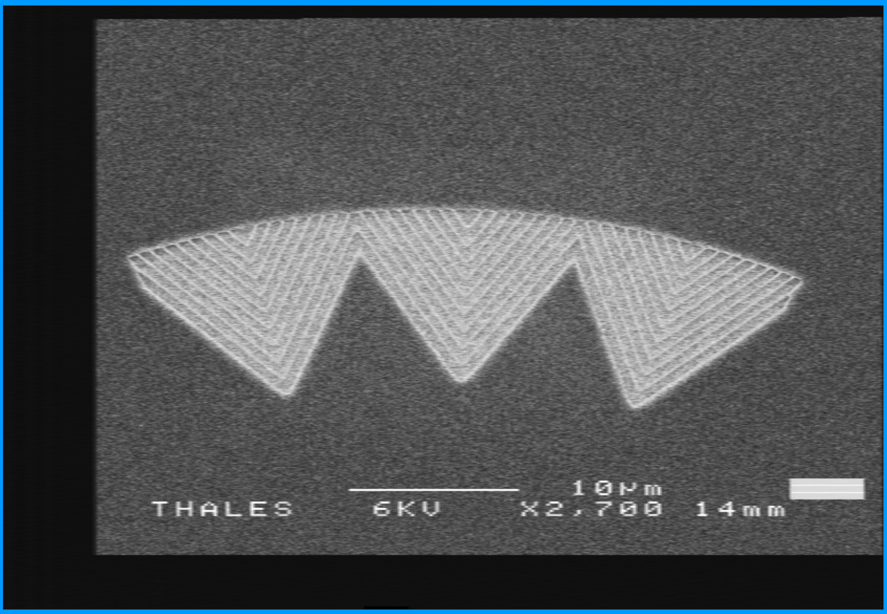

Proximity Effect Correction

(Data supplied by Thales Research & Technology)

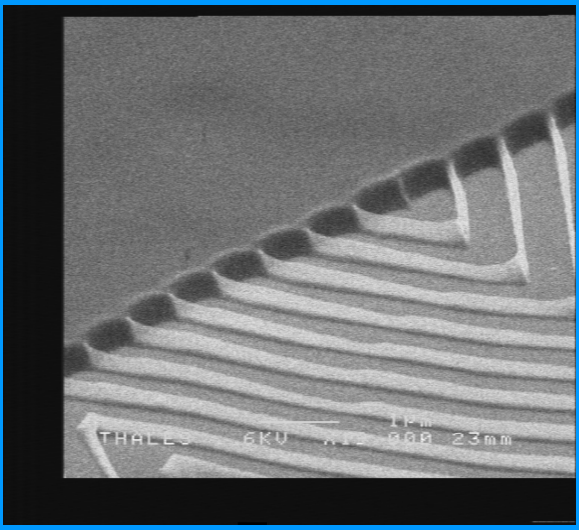

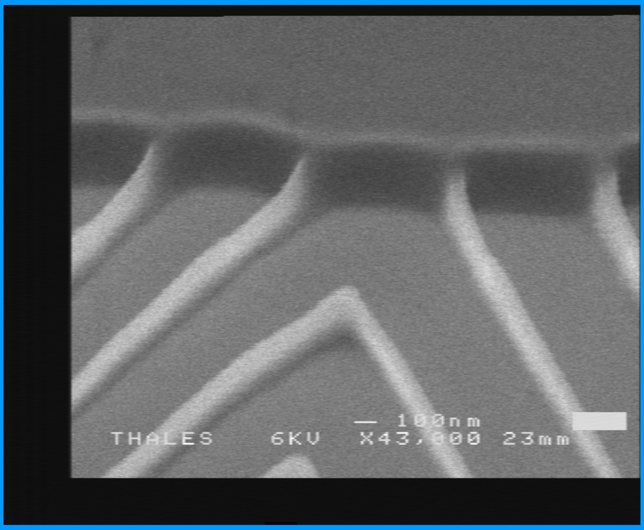

With proximity correction

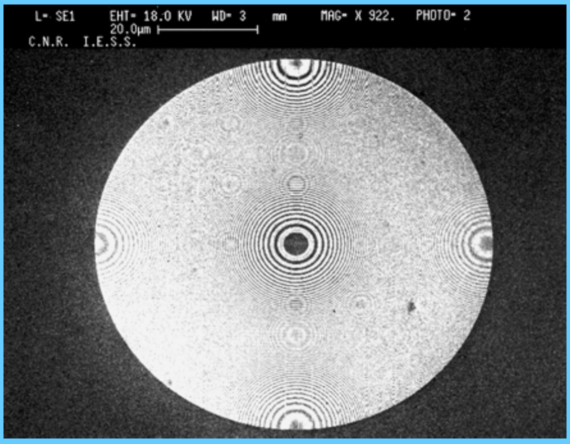

Without proximity correction

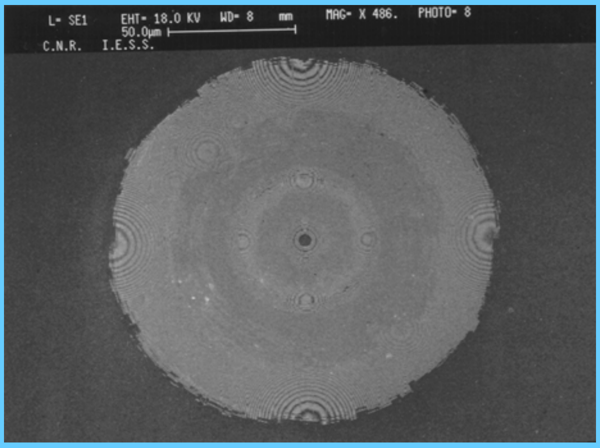

Diffractive Optical Elements

The E-Beam Lithography fabrication process of 3D profiles for phase DOEs

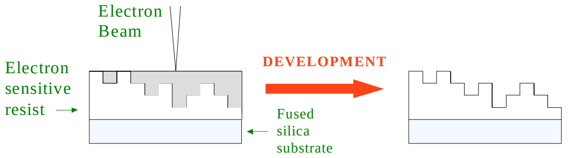

1- The phase profile is transferred by direct e-beam writing onto an electron sensitive resist (PMMA)

2- After the development, a surface relief pattern built in the resist can act as a DOE

CNR-IESS - µFab Group

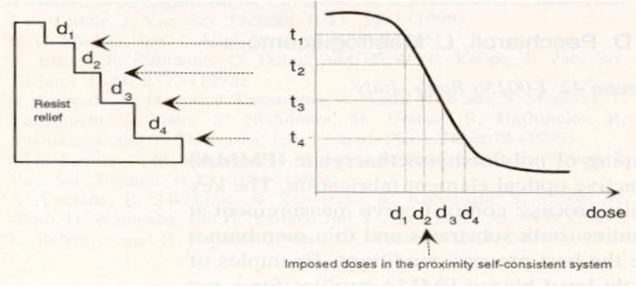

FIG. 1. Schematic description of dose assignment procedure.

The key for a good DOE efficiency

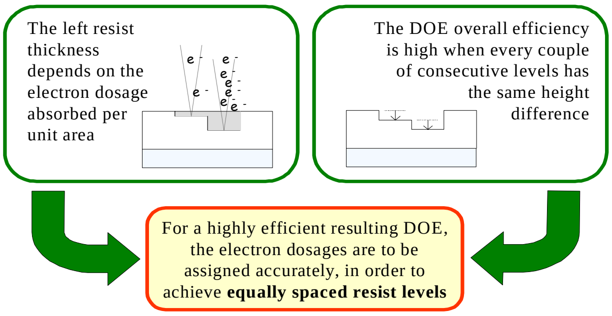

The left resist thickness depends on the electron dosage absorbed per unit area

The DOE overall efficiency is high when every couple of consecutive levels has the same height difference

For a highly efficient resulting DOE, the electron dosages are to be assigned accurately, in order to achieve **equally spaced resist levels**

CNR-IESS - µFab Group

The dose calibration

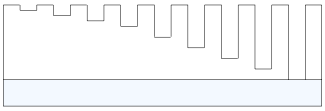

Resist pads are exposed at increasing electron dosages (the pad lateral size is larger than the electron backscattering range ⇨ the exposure dosage is equal to the absorbed dosage)

From the remaining resist thickness vs. absorbed dosage curve it is possible to interpolate the electron dosage values necessary to achieve determined resist thicknesses

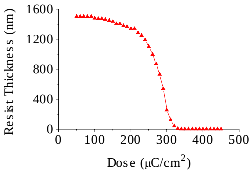

CNR-IESS - µFab Group

Continuous profiling

Normalized Resist Thickness vs. absorbed dosage curve obtained with **MiBK-IPA 3:1**

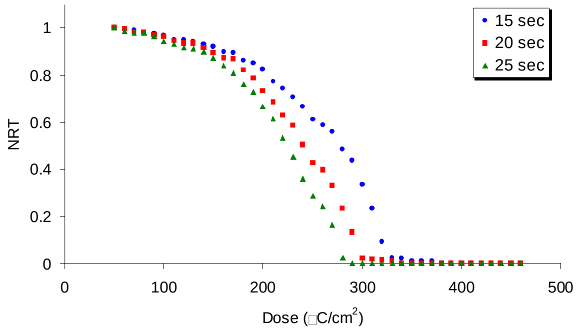

CNR-IESS - µFab Group

Testing the dose calibration on a practically realized multi-level profile

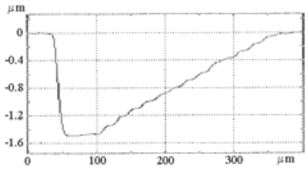

Profilometer measurements of the resist thickness performed on a 16-level ramp-shaped pattern.

Development: MiBK-IPA 3:1 for 20 sec.

The step width is 20 µm and their mean height is ~100 nm.
The maximum resist height is 1.5 µm.

Scanning Electron Microscope analysis

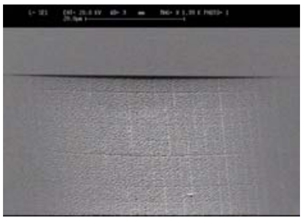

SEM image of a 16-level, 32 steps double ramp-shaped pattern.
Development: MiBK-IPA 3:1 for 20 sec.

Expected profile

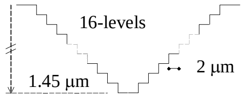

Applications of electron beam lithography

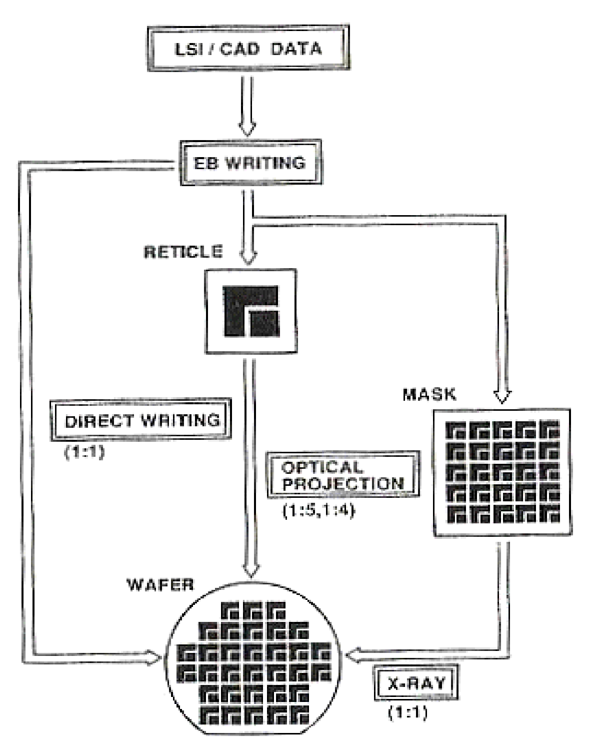

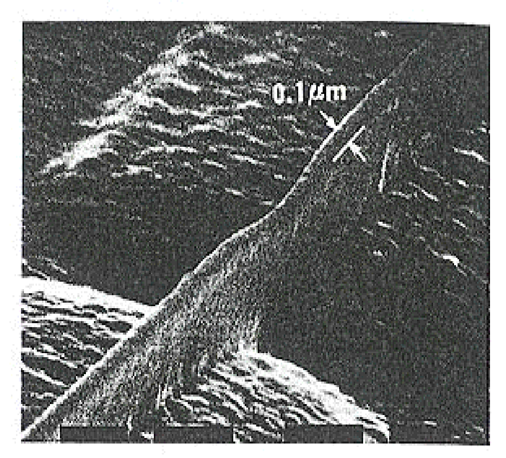

Mainly employed for the fabrication of photomasks

Also used to write patterns directly on wafer

L/S(Line & Space)Resist Pattern

HV : 30keV

Dose : 50µC/cm2

L/S = 50nm/70nm

L/S = 70nm/70nm

L/S(Line & Space)Resist Pattern

HV :   50keV

Dose : 140µC/cm2

L = 50nm P =100nm

L = 70nm P =140nm

L = 90nm P =200nm

L =150nm P =300nm

10 nm Space Width Resist Pattern

HV: 50kV

Resist : ZEP520

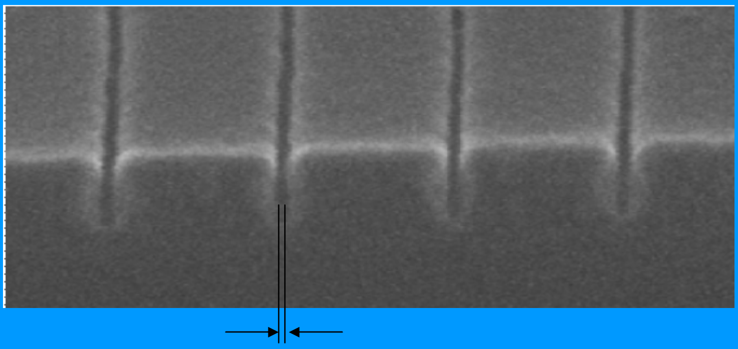

10 nm

Fabrication of Multi-Pitch Gratings

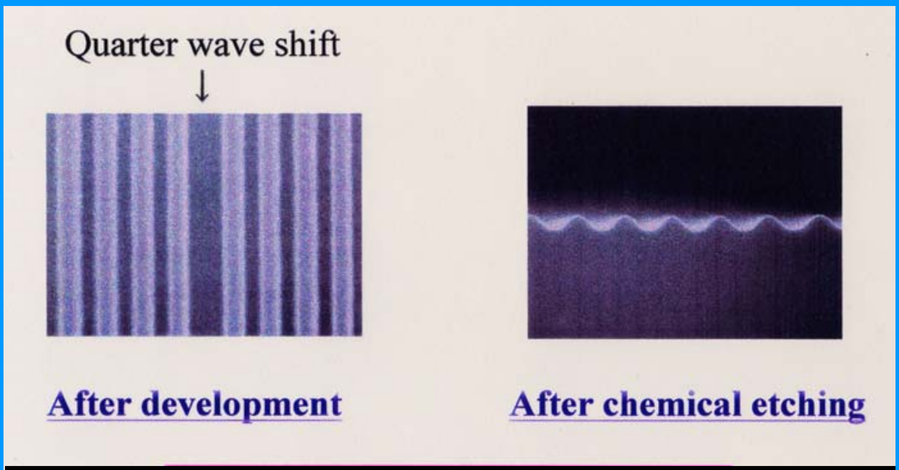

Grating Pitch : 235.98 ~ 247.68 nm

Spacing : 0.3 nm

Spot Scan Writing-Si Nanopillar for Photonic Crystal (by Spot Scan Writing)

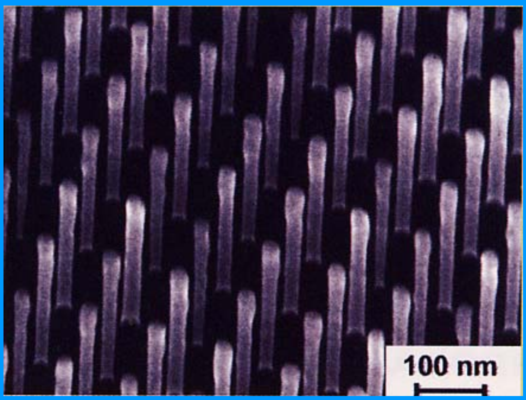

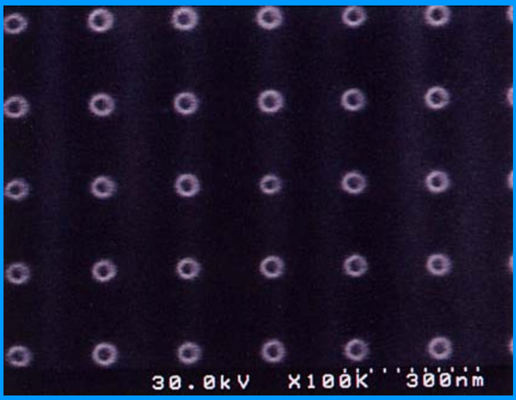

Nano-pillar

Dot array

The data supplied by Dr.T,Kanayama and Dr.T.Tada of JRCAT

Hexagonal Grating (by Spot Scan Writing)

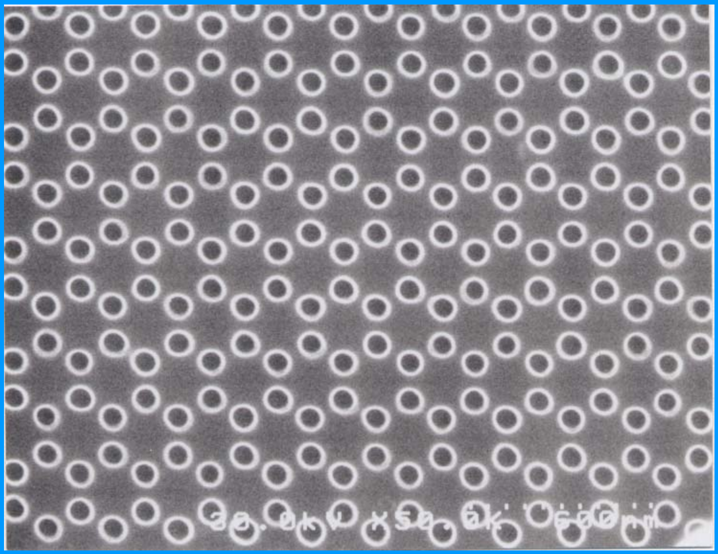

500 dots/100μm- length

30kV

5×10^{-11}A

40μs/dot

Photonic Crystal Waveguides by the Autocloning Technology

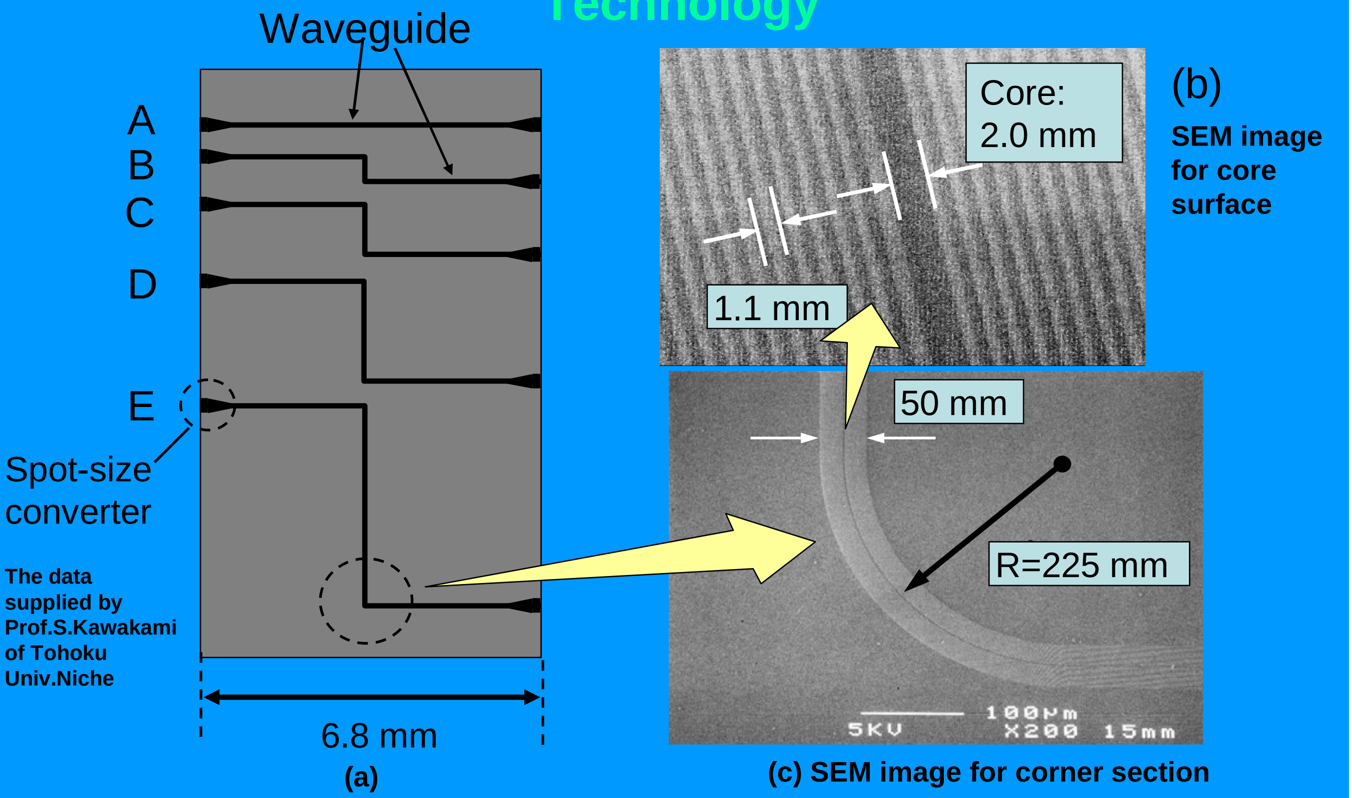

SEM image for core surface

The data supplied by Prof.S.Kawakami of Tohoku Univ.Niche

(a)

(c) SEM image for corner section

Blazed Grating

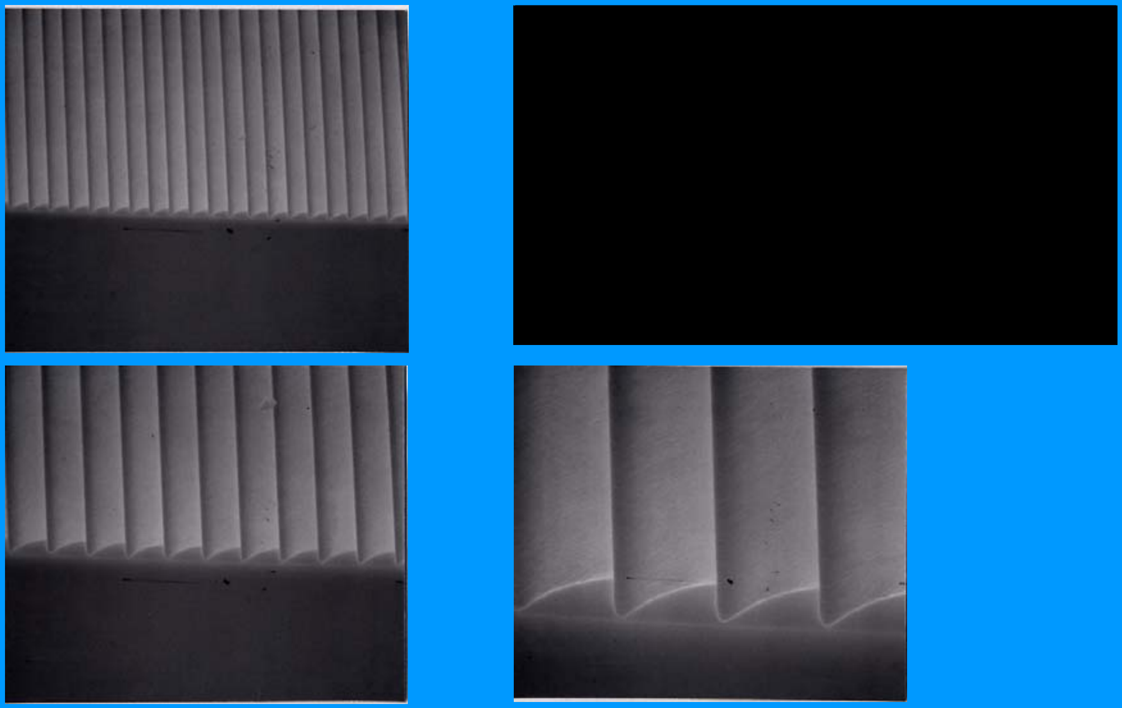

3-D Concentric Circular Pattern

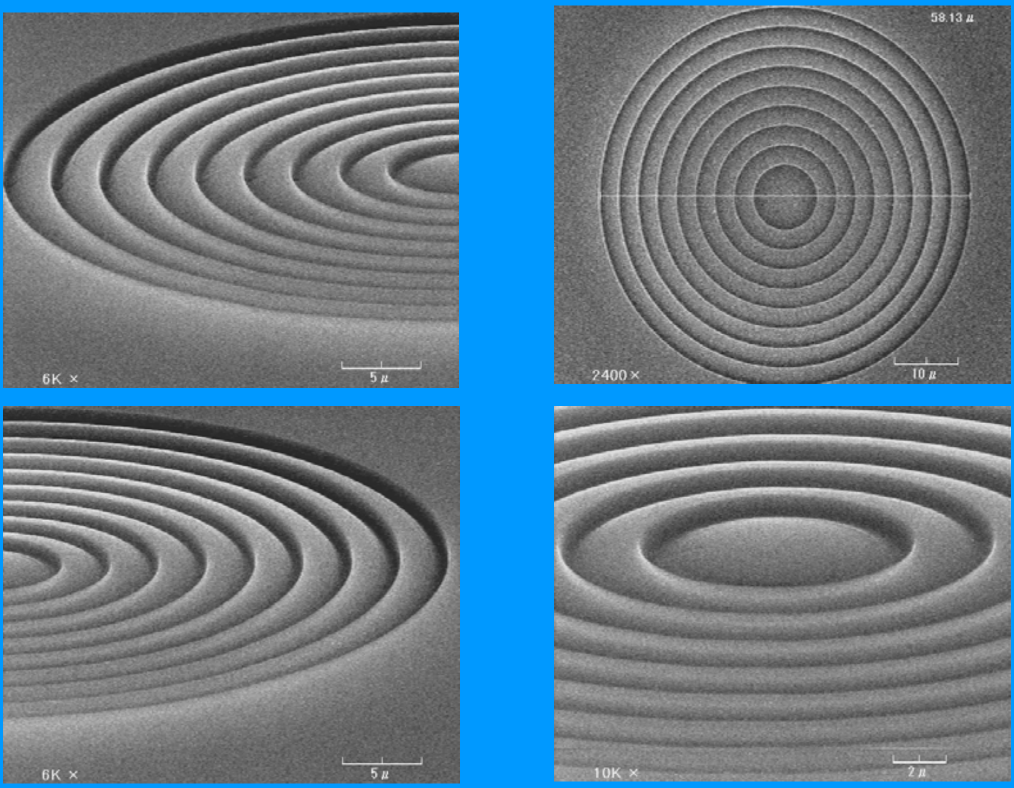

Continuous profile holographic surfaces produced by e-beam methods

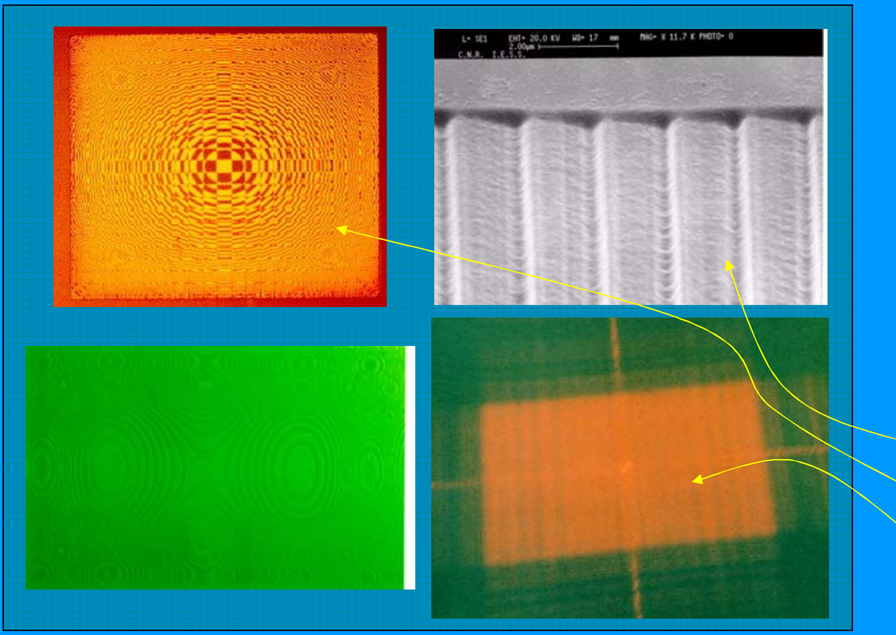

Continuous profile make it possible to design a wavefront transforming surface having the exact theoretical shape required to maximize efficiency.

- *Continuous profile*
- *Overall pattern*
- *Uniform redistribution of laser light obtained by the innovative optical element*

Ion Beam Lithography

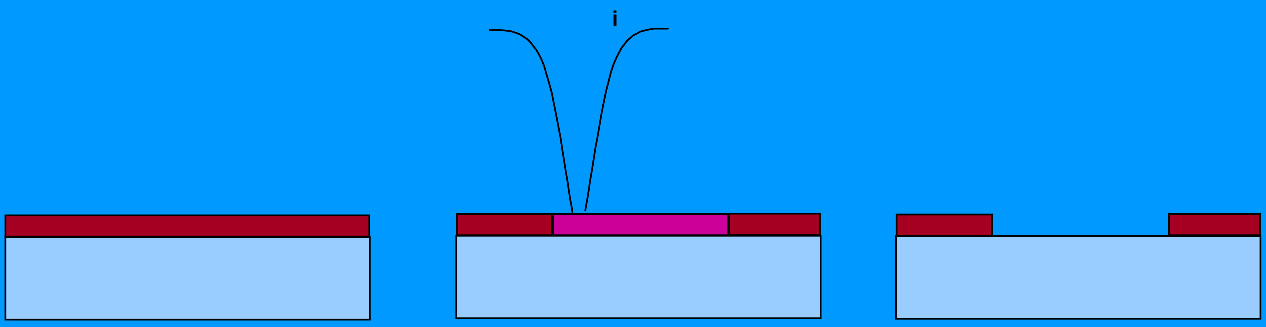

1) Casting of thin resist film

2) Ion beam patterning of resist

3) Development of resist

- Advantages of ion beams:
  - Enhanced resists sensitivity
  - Can be focused to narrower linewidth
  - Reduced Scattering
  - Allows hybrid processes such as ion-induced etching and implantation

More ? Google it !

Ion beam lithography techniques

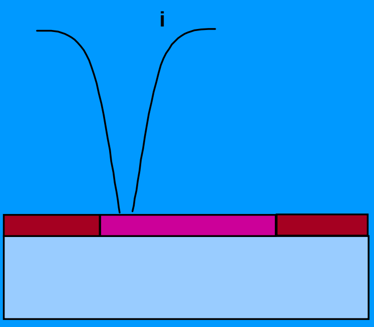

Focused Ion Beam Lithography (FIBL)

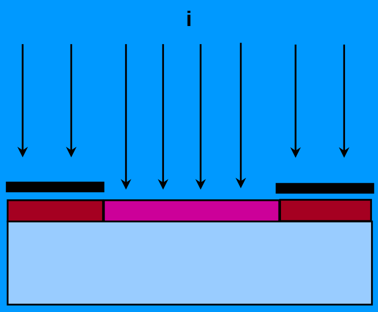

Masked Ion Beam Lithography (MIBL)

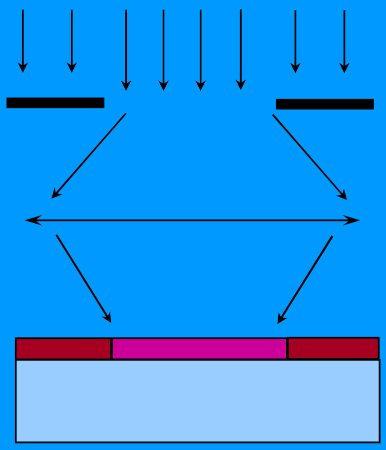

Ion Projection Lithography (IPL)

Focused Ion Beam Lithography

FIBL components:

- Ion source
- Ion optics column
- Sample displacement table

Specifications:

- Accelerating voltage 3-200 kV.
- Current density up to 10 A/cm^2 .
- Beam diameter 0.5-1.0 µm.
- Ions: Ga$^+$, Au$^+$,Si$^+$,Be$^+$ etc.

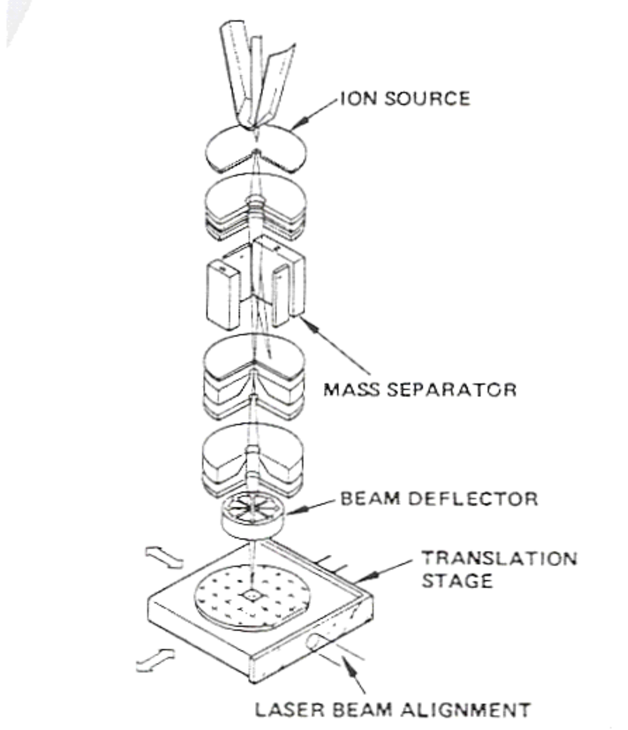

Ion optics

- Electrostatic lenses are employed due to large mass of ions
- Mass spectrometers are used to separate different species of ions

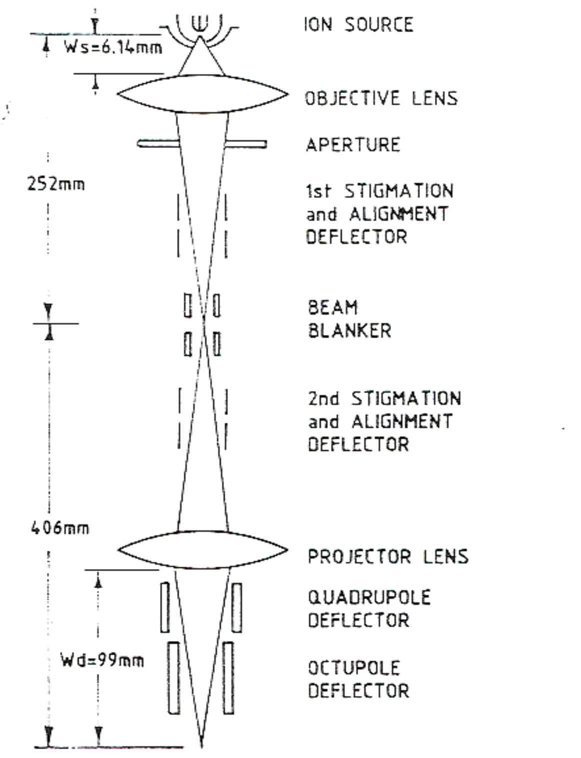

FIB fabricated nanostructures

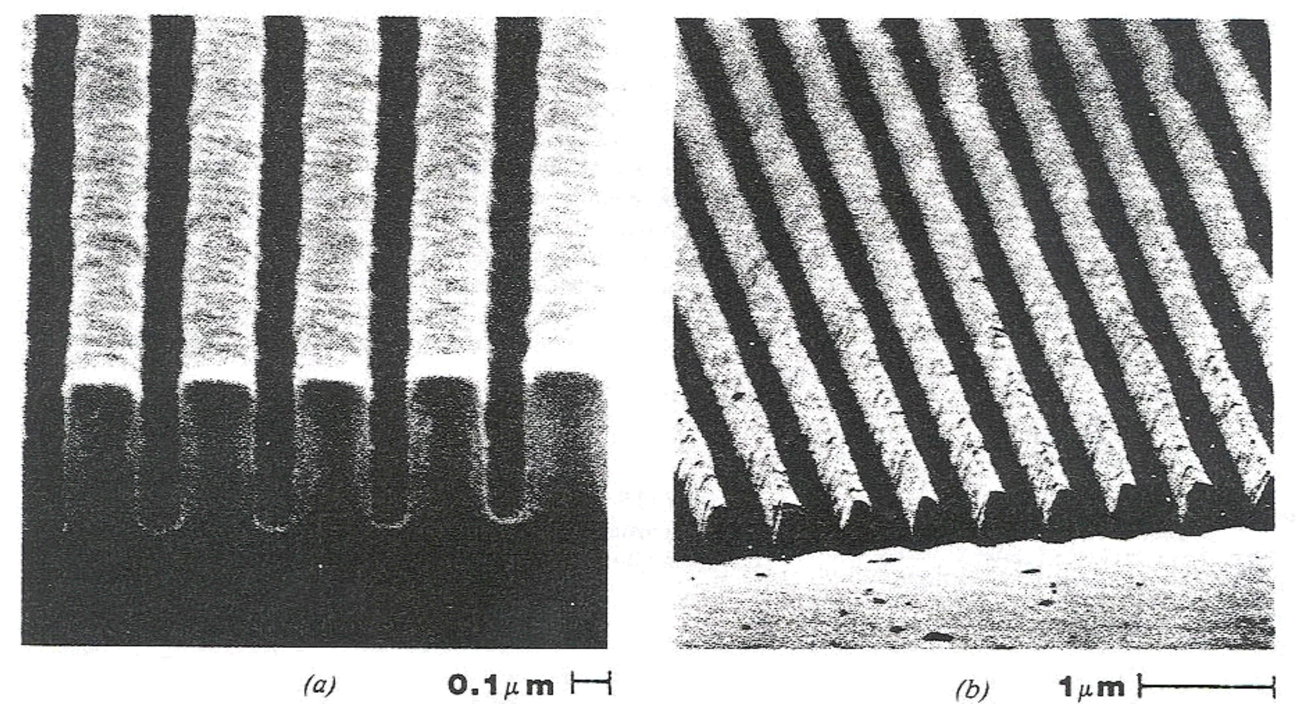

Ion projection lithography

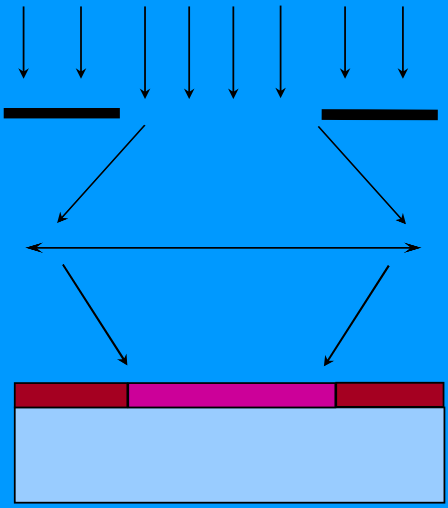

Ion Projection Lithography (IPL)

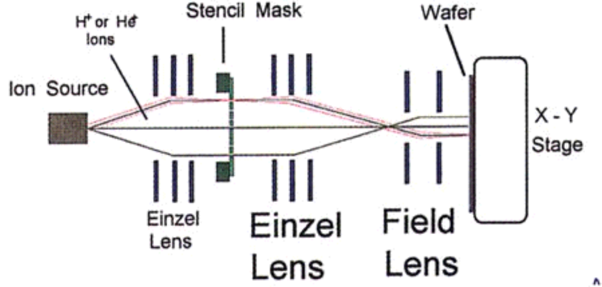

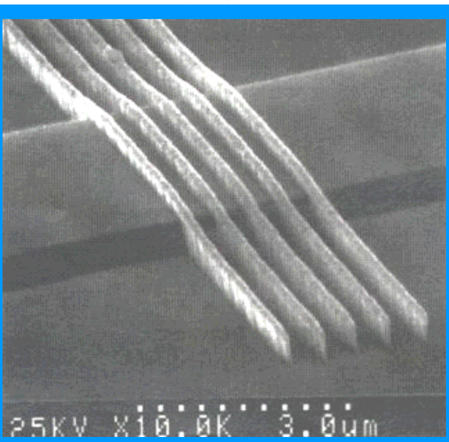

Source: The Advanced Lithography Group

Alternate Nanolithography Techniques

Alternate Nanolithography Techniques

- Micro-contact Printing
- Nanoimprint Lithography
- Scanned Probe Lithography
- Dip-pen Lithography

Micro-contact printing

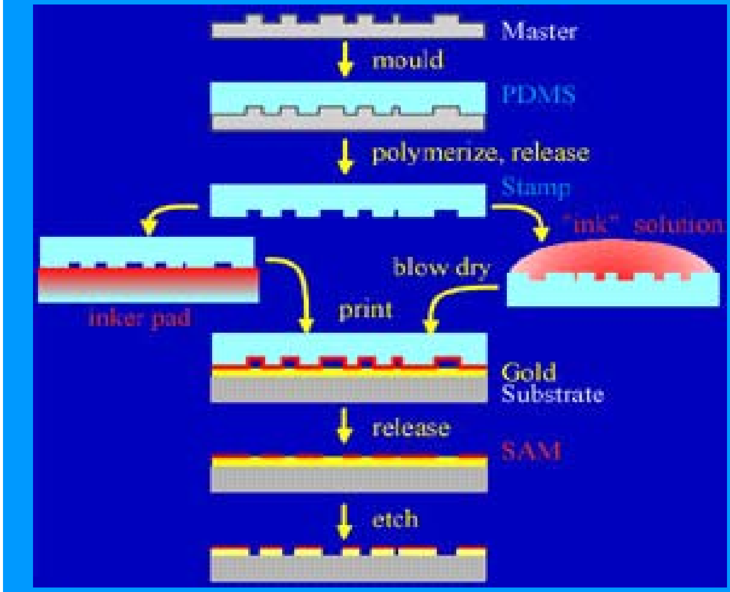

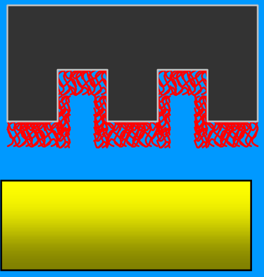

1) Application of ink to stamp

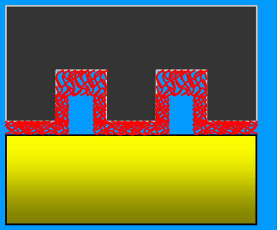

2) Application of stamp to surface

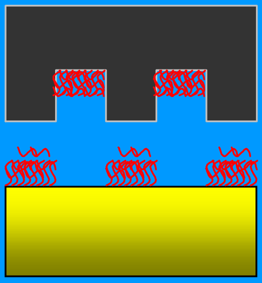

3) Removal of stamp

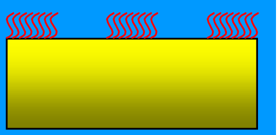

4) Residues rinsed off

Source: IBM Zurich

Micro-contact printing

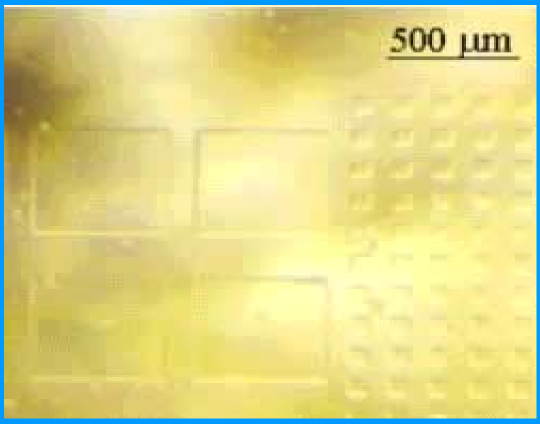

Printing of PDMS

Source: Winograd Group, Penn State

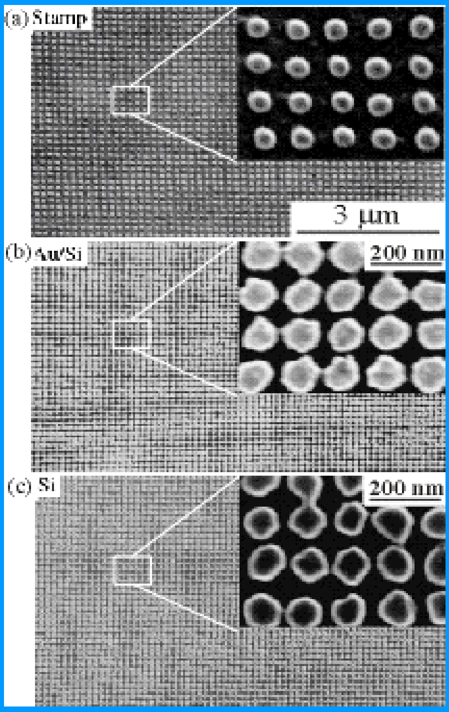

High-resolution µCP of 60 nm dots

Source: IBM Zurich

Nanoimprint Lithography

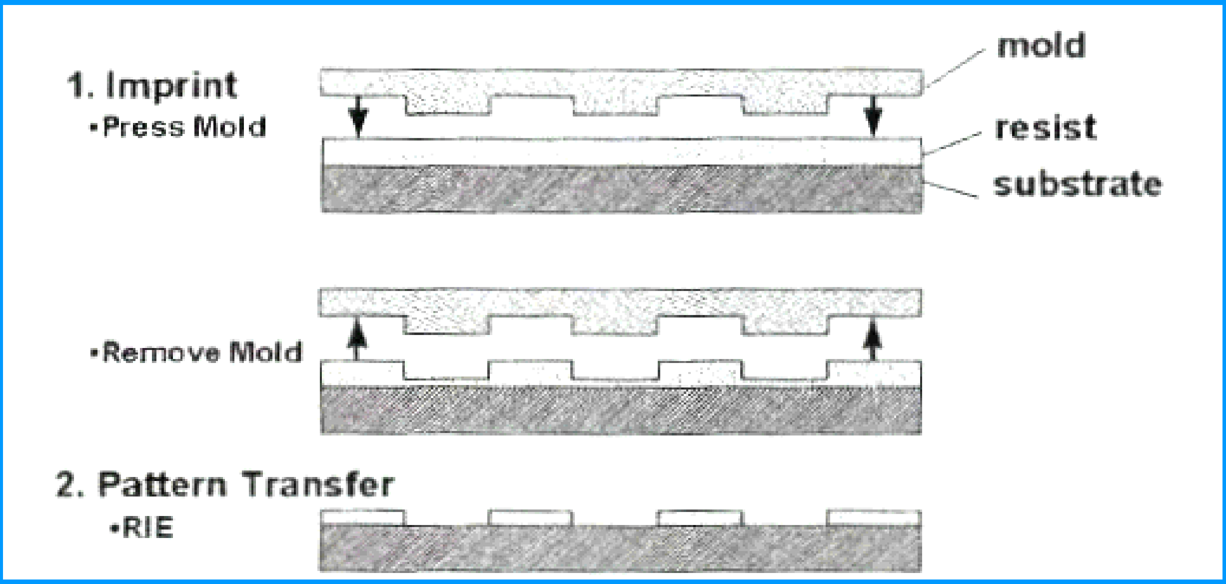

Consists of pressing a mold onto the resist above its glass transition temperature T_g

More ? Check out S. Y. Chou, Princeton

NIL master

- SiO_2 pillars with 10 nm diameter, 40 nm spacing, and 60 nm height fabricated by e-beam lithography.
- Master can be used tens of times without degradation

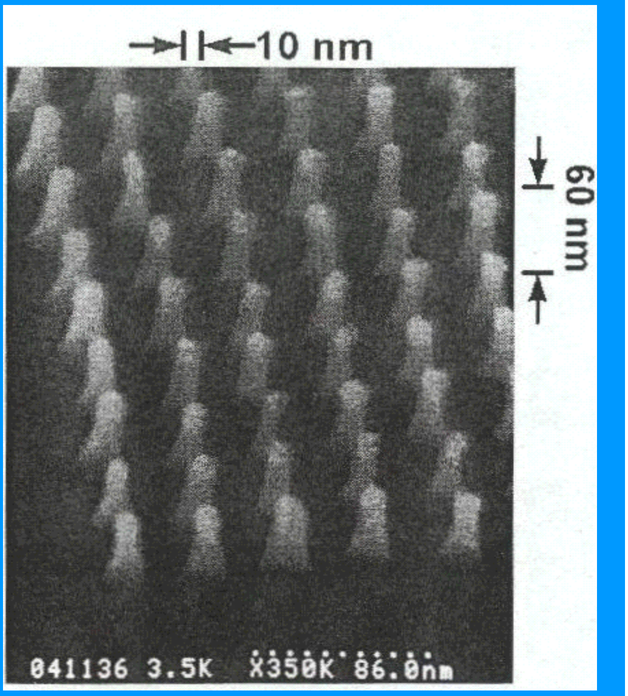

NIL pattern in PMMA

- Mask is pressed into 80 nm thick layer of PMMA on Si substrate at 175° C (T_g=105 ° C), P= 4.4 MPa.
- PMMA conforms to master patterng, resulting in ~10 nm range holes

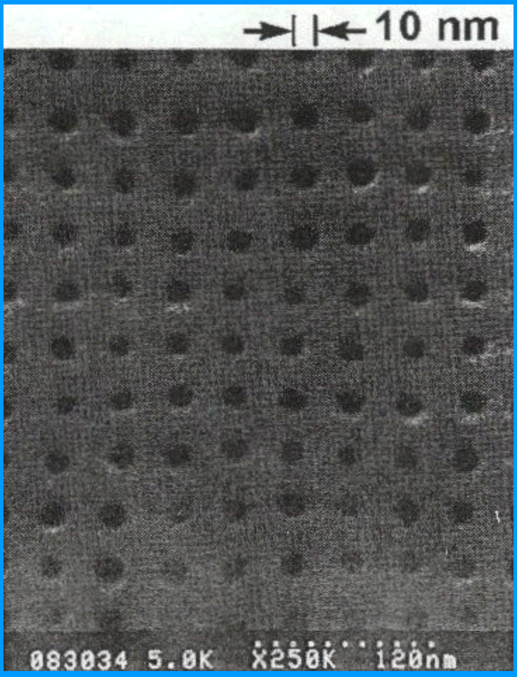

Carbon nanotubes for nanolithography

- A carbon nanotube can be used as a tip in an atomic force microscope (AFM). Such a tip in an AFM can be used to create nanoscale patterns i.e. nanolithograpghy or to etch material away from a surface in the fabrication of semiconductor chips
- The videoclips show real-time dynamics of interaction between carbon nanotube tips and silicon and surfaces

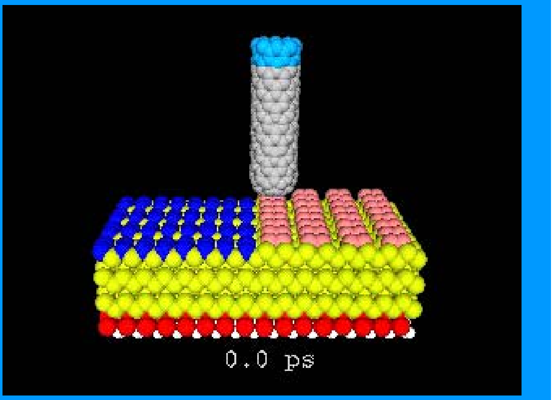

Ref: NASA, Ames Center

Carbon nanotubes for nanolithography

Preliminary simulation and experiment show:

- * the world’s tiniest and strongest nanopencil
- * never needs sharpening

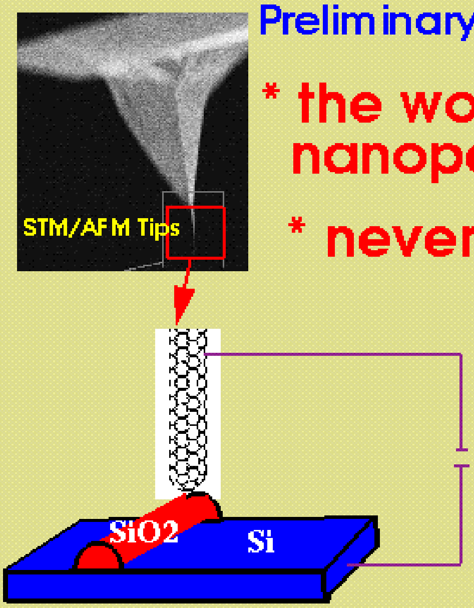

TEM Image: SiO2 lines (10 nm width) on Si Surface, writen by a CNT tip

Ref: NASA, Ames Center